Arabian Journal for Science and Engineering (2025) 50:11145–11166
https://doi.org/10.1007/s13369-024-09453-0

RESEARCH ARTICLE-SYSTEMS ENGINEERING

Navigating Process Drift: The Power of CUSUM in Monitoring Air Quality Processes and Maintenance Operations

Muhammad Riaz[1] · **Huda Alshammari**[1] · **Nasir Abbas**[1] · **Tahir Mahmood**[2]

Received: 4 January 2024 / Accepted: 11 July 2024 / Published online: 29 August 2024

Abstract

Nowadays, manufacturers face intense pressure to maintain a high standard of quality. Due to the damage to machine components, manufacturing processes degrade over time, resulting in substandard products. Generally, statistical process control tools such as control charts aid in identifying patterns and trends indicative of process changes. This investigation delves into the effectiveness of cumulative sum control charts using the sample mean and median as plotting statistics. Run-length measurements assess performance after the charts experience linear and quadratic drifts in non-normal setups under zero- and steady-state conditions. The findings reveal that Cumulative Sum (CUSUM) charts outperform zero-state monitoring compared to steady-state monitoring. Notably, the CUSUM chart for the mean is suitable for normal and Gamma distributions, exhibiting a greater ability for drift detection under biased and unbiased Average Run Lengths. This study offers valuable insights into enhancing manufacturing quality through effectively implementing and comparing Shewhart, Exponentially Weighted Moving Average, and CUSUM charts. By evaluating their performance under various conditions and comparing them with other control chart methods, this research provides valuable guidance for industries seeking to improve process monitoring and product quality. It is essential to acknowledge that the findings are based on specific experimental conditions and may not fully capture the complexity of real-world manufacturing environments. For practical purposes, the suggested charts are also applied to real-world case studies, including air quality (focusing on five metal oxide chemistry sensors: carbon monoxide concentration, non-metonic hydrocarbons, benzene, total nitrogen oxides, and nitrogen dioxide) and maintenance data (including air temperature, rotating speed, and equipment failure).

Keywords CUSUM · Linear drifts · Memory charts · Process monitoring · Quadratic drifts · Run length profile · Statistical process control

1 Introduction

Statistical process control (SPC) is a technique for monitoring and controlling a process or manufacturing method using seven popular instruments. SPC can assist in identifying issues and avoiding the development of faults in a process [1]. Walter A. Shewhart created SPC in the 1920s, and W. Edwards Deming popularized it in Japan following World War II. The core SPC tools, like control charts, are extensively used in industrial operations. Control charts are graphs that display the changes in a process variable over time. Control charts can establish whether a process is under statistical control and identify common and unique causes of variation [2]. Common cause variation is always present in processes, and special cause variation comes from outside sources, implying that the process is not under statistical control. Control charts are separated into two groups based on the parameter that needs to be examined.

In contrast to dispersion charts, which focus on the variability parameter, location charts, the topic of this article, are control charts that focus on the centrality parameter. In addition, there are two main kinds of control charts, depending on how severe the process disturbances are. Memoryless charts like Shewhart charts detect large, abrupt changes in processes. In contrast, memory charts like cumulative sum and exponentially weighted moving average control charts identify smaller changes that may not be easily detected.

✉ Muhammad Riaz
riazm@kfupm.edu.sa

[1] Department of Mathematics, King Fahd University of Petroleum and Minerals, 31261 Dhahran, Saudi Arabia

[2] School of Computing, Engineering and Physical Sciences, University of the West of Scotland, Paisley PA12BE, UK

Both types provide distinct insights into process variations, assisting in informed process improvement decision-making. The study will primarily focus on memory charts for location monitoring, specifically on the cumulative sum (CUSUM) control chart that was developed by Page [3].

CUSUM charts improve the ability to detect small changes, and the plotting statistic includes both the most recent and prior values of the data [4]. Furthermore, the CUSUM chart plots the cumulative sums of the deviations of sample values from a target value. The CUSUM chart requires two parameters: a reference value (k) and a decision limit (h). Setting the reference value (k) to half of the detected drift and the decision limit (h) to the threshold for declaring the process out-of-control (OOC). The CUSUM structure will be examined using sample mean ($\overline{X}$) and sample median ($\widetilde{X}$) statistics, which are typically used to track the location of a process. When compared to the traditional Shewhart chart, the CUSUM chart is more sensitive to smaller shifts and drifts in the process mean. Furthermore, many authors have looked into the CUSUM chart; recent relevant works and references can be found in Erem and Mahmood [5] and Abbas [6]. Chakraborti and Graham [7] gave an updated look at control charts that do not rely on specific distributions. They proposed new methods for quality control that work across different industries without needing to assume specific data distributions. Madrid-Alvarez et al. [8] introduced a control chart designed specifically for Gamma distribution. It ensures consistent performance in spotting changes in processes, which is helpful in industries where Gamma distributions are common. Özdemir et al. [9] presented a new control chart that uses fuzzy numbers to detect changes in processes. They tested it in a real-world scenario and found it to be better at spotting issues in complex manufacturing settings. In this study, we present a comprehensive analysis of the performance of CUSUM control charts under both linear and quadratic drifts for mean and median estimators, extending the traditional focus beyond normal process environments to include student's t and Gamma distributions. This dual drift consideration and inclusion of non-normal distributions represent a significant advancement over previous studies, which predominantly focused on single drift types and normal distribution assumptions. Furthermore, our research introduces practical applications of these charts, providing a detailed comparison with EWMA and Shewhart control charts. The identification of superiority zones for different control charts under various conditions is a novel contribution that aids in the precise selection of the most effective chart for specific monitoring scenarios.

Drift is a data pattern that denotes a slow, linear, or nonlinear change in the process mean over time. The most common causes include tool wear, chemical concentration, temperature, etc., that impact the process Reynolds and Stoumbos [10]. For instance, a classic sign of tool wear is when the size of the tool varies in comparison with its former size. Once the reason for the drift has been determined, the required action can be taken. Shift, linear drift, and quadratic drift are all considered in this study. The shift is characterized as a sudden increase or decrease in the performance of process. This shift can occur due to various factors, such as changes in market demand or modifications in production methods. The conventional shift in the mean is defined as$\mu_1 = \mu_0 + \delta\sigma_0$. Where μ_1 is the shifted mean, and δ is the amount of change times σ_0 in the process mean. Traditionally, δ stays constant across time. However, some processes experience deviations that occur gradually over time. The terms "drifts" and "trends" refer to the gradual change in the measurement readings over time, either linearly or nonlinearly. The formulas of the linear drift and the quadratic drift are $\mu_1 = \mu_0 + \omega t\sigma_0$ and $\mu_1 = \mu_0 + \rho t^2\sigma_0$, respectively, where μ_1 is the drifted mean, and (ω, ρ) are the amount of change times σ_0 in the process mean, and t represents the time point.

The performance of the control chart was investigated from a variety of perspectives in the SPC literature. For instance, Bissell [11] proposed a CUSUM chart for monitoring trends. Also, Bissell [12] expanded the Markov chain methodology by examining the run-length characteristics of the Shewhart and CUSUM charts. Aerne et al. [13] evaluated how the Shewhart, CUSUM, and EWMA charts performed when there was a linear drift in the process mean. Gan [14] examined the EWMA performance of chart while there was linear drift. Davis and Krehbiel [15] investigated the role of X control charts with run-rules in the presence of a linear trend in the process mean. The findings show that a run-rules-based control chart outperforms an X control chart when a linear trend in the process mean is included. Bücher et al. [16] studied a method called Cumulative Sum Change-Point Detection Tests, which combines different tests to see if there are any shifts or changes in the data pattern. Hou and Yu [17] introduced a method to detect and understand changes in manufacturing processes. Their approach, called non-parametric CUSUM control chart, helps factories identify different types of changes more accurately without needing to assume specific data patterns. Diko et al. [18] suggested improvements to a two-sided CUSUM chart. This tool makes the CUSUM structure more accurate, especially when certain parameters need to be estimated. Haq and Ali [19] presented a method called maximum dual CUSUM chart, which helps monitor both the average and variability of processes simultaneously. This approach improves quality control by allowing quicker detection of any changes in the process mean and/or variance.

Gültekin et al. [20] evaluated the effectiveness of cross-correlation charts with various control charts on processes with a mean subject to linear drift. The proposed chart outperforms both the CUSUM and the X trend control charts.

Fahmy and Elsayed [21] compared the performance of Shewhart, CUSUM, EWMA, and generalized likelihood ratio (GLR) control charts with that of the chi-square chart, which seeks to identify linear trends in the process mean. Shu et al. [22] investigated the performance of the weighted CUSUM chart under the influence of linear drifts. In order to detect linear drifts, Zou et al. [23] compared the effectiveness of control charts such as generalized likelihood ratio (GLR), EWMA, CUSUM, and generalized EWMA (GEWMA). Their findings demonstrated that the GLR-based control chart worked better than the other charts taken into account. Yi and Qiu [24] introduced a special CUSUM chart that is good at spotting drifts in processes. It adapts to changes in data patterns, making it useful for catching both sudden and gradual shifts in quality control. Mejri et al. [25] suggested a new chart to identify the presence of drifts in processes. This chart adjusts its limits over time to notice changes in data patterns, helping maintain process stability by spotting problems early. Mou et al. [26] proposed a new method to track changes in Poisson rates over time. Their method is good at detecting gradual changes, even when the number of samples varies, helping maintain process quality. Capizzi and Masarotto [27] discussed making control charts that always work well even when parameters are estimated. Their work emphasizes the need for strong monitoring systems to catch changes in process parameters early.

Assareh et al. [28] used a Bayesian framework to describe and locate the transition point, assuming that the underlying change was a linear trend in the odds ratio of a Bernoulli process. Atashgar, Noorossana [29] proposed an artificial neural network-based approach for a bivariate environment with linear trend disruption. Furthermore, to better evaluate linear mean drift, Xu et al. [30] proposed using a control chart based on a GLR to assess the linear mean drift. Recent proposals by Yi and Qiu [31] for a new drift detection technique, utilizing the general framework, the new method generates a CUSUM chart based on the GLR statistics. It is clear from the studies mentioned above that a lot of studies employ $\overline{X}$ chart to investigate the effects of shifts and linear drifts in the data. As far as the authors are aware, drifts are not considered in relation to $\widetilde{X}$ charts. Additionally, while location-based research is addressed under the subject of linear drift over time, there is relatively less literature available on the detection of quadratic drifts. Centofanti et al. [32] developed a functional regression control chart for monitoring quality profiles in industrial processes. This method adjusts for covariate effects using residuals from a function-on-function linear regression, providing advantages in detecting shifts in covariate means, which is crucial for maintaining process control. Lefebvre and Miller [33] explored stochastic delayed control problems within a linear-quadratic framework and introduced a deep learning scheme for addressing control delays. Their approach offers insights into improving process control, particularly in handling delays that affect the performance of CUSUM control charts. Han et al. [34] studied robust time-inconsistent stochastic linear-quadratic control, focusing on managing worst-case drift disturbances. Their work emphasizes deriving equilibrium controls, which enhance robustness in process control scenarios, relevant for improving CUSUM and EWMA control chart performance. Li et al. [35] adopted a reinforcement learning method to solve stochastic linear-quadratic control problems, highlighting an online RL algorithm for optimal control with partial system information. This approach simplifies the calculation process and can be applied to enhance the effectiveness of CUSUM control charts in real-time monitoring. Marais et al. [36] compared various control charts, including Shewhart, CUSUM, and EWMA charts, for fault detection in wastewater treatment. Their study found that EWMA charts performed best for drift faults, underscoring the importance of selecting the appropriate control chart for different fault characteristics. De Oliveira et al. [37] developed ARMA-based control charts for fault detection and diagnosis in batch processes. Their integration of time series models to capture variability in both time and batch domains offers improvements in monitoring batch process dynamics, relevant for enhancing CUSUM chart applications. Sepp and Rakhmonov [38] introduced a log-normal stochastic volatility model with quadratic drift for the arbitrage-free valuation of options. Their work demonstrates the application of quadratic drift models, which is significant for extending CUSUM control chart methodologies to more complex process monitoring scenarios.

The purpose of this study is to comprehensively assess the performance of cumulative sum (CUSUM) control charts based on the sample mean ($\overline{X}$) and sample median ($\widetilde{X}$) across a range of practical scenarios. Specifically, we investigate the effectiveness of these charts in detecting shifts, linear drifts, and quadratic drifts in both normal and non-normal process environments. Additionally, we explore the impact of various subgroup sizes on the performance of the charts under zero-state and steady-state monitoring conditions. By conducting this thorough analysis, we aim to provide insights into which chart is better suited for effectively spotting process fluctuations in different settings, thereby addressing a crucial gap in the literature on process monitoring methods. The following would be how the rest of the content is arranged: Sect. 2 provides a description of the control chart structure for location monitoring. Section 3 contains a design for the suggested charts. Section 4 reports the results of the performance assessment of charts. Two real-life examples of how the suggested charts can be used in practice are described in Sect. 5. In Sect. 6, a comparative analysis under drifts is provided. In Sect. 7, comments and suggestions for future research are given.

2 Control Charts for Location Monitoring

This section is designed to discuss the general structure of cumulative sum control charts based on sample mean ($\overline{X}$ − CUSUM) charts and cumulative sum control charts based on sample median ($\widetilde{X}$ − CUSUM) control charts.

2.1 $\overline{X} - CUSUM$ Chart

Suppose $X_{t,i}$ where $i = 1,2\ldots, n$ and $t = 1,2, \ldots,$ are independent, randomly distributed variables that follow a normal distribution with an n-sample size, i.e.,$X_t \sim N(\mu_0 + \delta t\sigma_0, \sigma_0)$ where μ_0 and σ_0 are the in-control mean and standard deviation, respectively. Additionally, δ represents the magnitude of the standardized mean shift, and t stands for time; if $t = 1$, that indicates a consistent shift in the process mean. The process is under control if $\delta = 0$; otherwise, it is out-of-control.

The plotting statistic of $\overline{X}$ − CUSUM is given as follows:

$$C_t^- = \min[0, \left(\overline{X}_t - \mu_0\right) + k\left(\frac{\sigma_0}{\sqrt{n}}\right) + C_{t-1}^-] \tag{1}$$

$$C_t^+ = \max\left[0, \left(\overline{X}_t - \mu_0\right) - k\left(\frac{\sigma_0}{\sqrt{n}}\right) + C_{t-1}^+\right] \tag{2}$$

with $C_0^+ = C_0^- = 0$ and k is the reference value, also known as the sensitive parameter. The parameter k is determined to represent one half of the magnitude of the intended shift, i.e., $k = \frac{|\delta|}{2}$. The sample mean $\overline{X}_t$ is defined as

$$\overline{X}_t = \frac{\sum_{i=1}^{n} X_{t,i}}{n} \tag{3}$$

The Lower and Upper Control Limits (LCL and UCL, respectively), which are provided as follows, are plotted against the plotting statistic of $\overline{X}$ − CUSUM.

$$\text{LCL} = h_1\left(\frac{\sigma_0}{\sqrt{n}}\right) \tag{4}$$

$$\text{UCL} = h_2\left(\frac{\sigma_0}{\sqrt{n}}\right) \tag{5}$$

where the central line is CL = μ_0 and h_1 and h_2 are charting constants calculated with respect to $\text{ARL}_0 = 370$ and listed in Table 1. The process stability is dependent on maintaining the LCL and UCL values. Thus, $\overline{X}$ − CUSUM chart will signify any change if ${C_i}^+$ exceeds the UCL or ${C_i}^-$ is plotted below LCL, and the process is said to be unstable.

3 $\widetilde{X} - CUSUM$ chart

Let $X_{t,i}$; $i = 1,2\ldots, n$; $t = 1,2, \ldots$ be a normally distributed t^{th} subgroup of size$n$, i.e.,$X_t \sim N(\mu_0 + \delta t\sigma_0, \sigma_0)$. The t^{th} plotting statistic of the $\widetilde{X}$ − CUSUM chart is stated as follows:

$$C_t^- = \min[0, \left(\widetilde{X}_t - \mu_0\right) + k\sigma_0\sqrt{\left(\frac{\pi}{2n}\right)} + C_{t-1}^-] \tag{6}$$

$$C_t^+ = \max\left[0, \left(\widetilde{X}_t - \mu_0\right) - k\sigma_0\sqrt{\left(\frac{\pi}{2n}\right)} + C_{t-1}^+\right] \tag{7}$$

with $C_0^+ = C_t^- = 0$ and k is the reference value, and $\widetilde{X}_t$ is expressed as

$$\tilde{X}_t = \begin{cases} X_{t,\left(\frac{n+1}{2}\right)}, & \text{if } n \text{ is odd} \\ \frac{X_{t,\left(\frac{n}{2}\right)} + X_{t,\left(\frac{n}{2+1}\right)}}{2}, & \text{if } n \text{ is even} \end{cases}, \tag{8}$$

where the t^{th} ordered subgroup represented by $X_{t,(1)}, \ldots, X_{t,(n)}$. See Maritz, Jarrett [39] for details about the variance of the sample median. The control limits are as follows:

$$\text{LCL} = h_1\sigma_0\sqrt{\left(\frac{\pi}{2n}\right)} \tag{9}$$

$$\text{UCL} = h_2\sigma_0\sqrt{\left(\frac{\pi}{2n}\right)} \tag{10}$$

where h_1 and h_2 are charting constants for the $\widetilde{X}$ − CUSUM chart. Table 1 consists of the values of the decision limits against the fixed ARL_0=370. A signal is generated by the $\widetilde{X}$ − CUSUM chart if ${D_t}^+$ exceeds the UCL or ${D_t}^-$ is plotted below LCL; else, the process is said to be in-control (IC).

4 Design of Simulation Study

Run length (RL) is a regularly used technique in statistical process control to study, track, and evaluate the effectiveness of the chart in identifying changes in a process [40]. By precisely measuring the run length, valuable insights can be gained, enabling better decision-making of processes. In addition, the standard performance metric is employed to assess a chart based on run length (RL), including average run length (ARL). The ARL measure is the average number of observations before a specific change occurs. This measure is used to monitor and detect any deviations or abnormalities in a process at a specific moment. ARL is divided into two categories in performance evaluation: (i) ARL_0 is the average run length in the IC state, and (ii) ARL_1 is the average run length in the OOC state. The control chart with a lower value of

Table 1 Charting constants of the $\overline{X}-$ CUSUM and $\widetilde{X}-$ CUSUM chart against fixed ARL_0=370

Chart	Distribution	$n=5$		$n=7$		$n=10$	
		h_1	h_2	h_1	h_2	h_1	h_2
$\overline{X}$	Normal	−2.24	2.24	−1.865	1.865	−1.5	1.5
	Student's t	−2.95	2.95	−2.49	2.49	−2.01	2.01
	Gamma	0.914	3.59	0.773	2.998	0.623	2.42
$\widetilde{X}$	Normal	−6.08	6.08	−5.26	5.26	−4.05	4.05
	Student's t	−5.7	5.7	−4.62	4.62	−3.26	3.26
	Gamma	1.35	9.34	1.23	7.6	0.985	5.44

ARL_1 is thought to be more effective when the $ARL_0 = 370$ [41]. Thus, the performance of the CUSUM charts will be assessed using the ARL as a performance metric.

In this study, the term "monitoring states" was used several times, and it refers to the two phases of continuously monitoring and assessing process behavior. These states include zero-state, where the change appears at the start of the operation, and steady-state, where the change appears after a specified amount of time; see Abbas [6] for more details. In this study, both zero-state and steady-state are used to evaluate the performance of the $\overline{X}-$ CUSUM and $\widetilde{X}-$ CUSUM control charts, with steady-state accounting for changes after the 50th point.

This study is designed by simulating various scenarios in which steady-state, zero-state, and different distributional settings are all incorporated into the simulation. Such as the normal distribution with a mean of zero and a variance of one (i.e., $N(0,\ 1)$), the student's t distribution with four degrees of freedom (i.e., t_4), and the Gamma distribution (i.e., Gamma(1, 1)). In our study, the t_4 distribution was chosen to examine heavy-tailed scenarios, such as irregular pollution events in air quality monitoring. The Gamma (1,1) distribution was selected to assess skewed data, such as equipment failure patterns in maintenance data. The size of the subgroups considered $n = 5$, 7, and 10. The study tries to capture any potential changes in the detection power of the chart during monitoring. Also, it will be determined how well the $\overline{X}-$CUSUM and $\widetilde{X}-$CUSUM charts perform when there is a regular shift, linear drift, and quadratic drift.

4.1 Algorithm for Control Charting Constants

The R language program is employed to determine the appropriate values for the charting coefficients. For the said purpose, the following steps were used:

Step 1: Set the values for the designed charts at a fixed ARL_0=370 throughout this procedure. The reference value is set to be $k = 0.5$, the amount of change $\delta = 0$, and change point $\tau = 0$ and subgroup size ($n = 5$, 7, and10).

Step 2: Generate a subgroup of size n with a normal distribution using ($\mu = 0, \sigma = 1$). However, when a subgroup is generated from the student's t distribution, then four degrees of freedom is used, while for the Gamma distributed subgroup, $\alpha = 1$ and $\beta = 1$ are used.

Step 3: Calculate the sample mean and sample median (i.e., $\overline{X}$ and $\widetilde{X}$) to compute the $\overline{X}-$ CUSUM given in Eqs. (1–2) and $\widetilde{X}-$ CUSUM provided in Eqs. (6–7) plotting statistics. The starting values for both plotting statistics are considered equal to zero.

Step 4: Set any arbitrary values for the charting coefficients (h_1 and h_2). Following that, the control limits of charts are determined.

Steps 1 through 4 are carried out in the R language software using 1,00,000 iterations to calculate the ARL_0 value. The procedure is repeated until the intended value of ARL_0 is obtained. When h_1 and h_2 are properly chosen, the ARL_1 performance of the proposed charts will be evaluated against δ values where $\delta = 0.01,\ 0.025,\ 0.05,\ 0.1,\ 0.25,\ 0.5,\ 1,\ 2,$ and4.

5 Results and Discussion

In this section, we examine how well the $\overline{X}-$ CUSUM and $\widetilde{X}-$CUSUM control charts perform when subjected to shifts and drifts. Table 2 provides a summary of the performance of the $\overline{X}-$ CUSUM and $\widetilde{X}-$ CUSUM charts based on zero-state monitoring. While the performance of the charts under a steady-state run length in the presence of shift, linear drift, and quadratic drift is summarized in Table 3. Tables, which take into consideration the various distributions, show the ARL values at fixed, $ARL_0 = 370$.

5.1 Zero-State Run Length Performance

In this section, the discussion will be about the evaluation of the performance of $\overline{X}-$ CUSUM and $\widetilde{X}-$ CUSUM under zero-state monitoring. The evaluation will be done by comparing the ARL_1 values to various values of δ. A

Table 2 Zero-state ARL profile of $\overline{X}-$ CUSUM and $\widetilde{X}-$ CUSUM charts when $n = 5$, 7, and 10

Chart	Distribution	δ	Shift			Linear drift			Quadratic drift		
			$n = 5$	$n = 7$	$n = 10$	$n = 5$	$n = 7$	$n = 10$	$n = 5$	$n = 7$	$n = 10$
$\overline{X}$	Normal	0	370.16	370.68	370.87	370.83	370.96	370.97	370.50	370.40	370.43
		0.01	367.22	368.70	369.42	40.59	38.51	36.51	9.67	9.17	8.71
		0.025	357.08	357.84	357.26	21.46	20.17	18.96	6.73	6.35	5.99
		0.05	324.10	319.88	319.02	13.21	12.30	11.47	5.13	4.82	4.52
		0.1	232.08	223.13	214.01	8.20	7.56	6.94	3.93	3.68	3.44
		0.25	63.27	55.49	47.97	4.46	4.03	3.64	2.82	2.65	2.42
		0.5	11.55	9.18	7.11	2.87	2.57	2.28	2.08	1.98	1.93
		1	2.73	2.09	1.60	1.91	1.71	1.47	1.87	1.71	1.47
		2	1.13	1.02	1.00	1.13	1.02	1.00	1.13	1.02	1.00
		4	1.00	1.00	1.00	1.00	1.00	1.00	1.00	1.00	1.00
	Student's t	0	370.94	370.65	370.14	370.63	370.97	370.82	370.03	370.70	370.42
		0.01	367.57	370.76	368.53	36.87	35.02	32.88	8.99	8.50	8.01
		0.025	361.03	364.54	358.40	19.00	17.77	16.56	6.27	5.90	5.52
		0.05	337.12	336.46	329.00	11.58	10.72	9.88	4.81	4.51	4.18
		0.1	256.48	247.31	228.87	7.18	6.56	5.97	3.74	3.47	3.15
		0.25	53.85	45.11	35.86	3.96	3.55	3.16	2.75	2.45	2.14
		0.5	6.70	5.11	3.77	2.61	2.28	2.00	2.00	1.97	1.92
		1	2.06	1.57	1.18	1.84	1.53	1.18	1.84	1.53	1.18
		2	1.02	1.00	1.00	1.01	1.00	1.00	1.01	1.00	1.00
		4	1.00	1.00	1.00	1.00	1.00	1.00	1.00	1.00	1.00
	Gamma	0	370.81	370.60	370.06	370.13	370.98	370.58	370.86	370.35	370.51
		0.01	405.60	404.32	397.65	50.11	47.10	44.14	10.76	10.14	9.55
		0.025	441.49	442.73	427.93	25.99	24.22	22.47	7.50	7.02	6.56
		0.05	460.32	451.62	428.00	15.80	14.59	13.41	5.73	5.36	4.98
		0.1	381.11	359.91	330.64	9.74	8.88	8.06	4.44	4.08	3.79
		0.25	136.17	117.18	97.85	5.30	4.75	4.24	3.07	2.90	2.76
		0.5	23.36	17.81	13.27	3.44	3.04	2.69	2.51	2.10	1.98
		1	4.05	3.03	2.21	2.26	1.96	1.81	1.98	1.94	1.81
		2	1.65	1.16	1.00	1.65	1.16	1.00	1.65	1.16	1.00
		4	1.00	1.00	1.00	1.00	1.00	1.00	1.00	1.00	1.00
$\widetilde{X}$	Normal	0	370.72	370.98	370.09	370.40	370.16	370.77	370.02	370.47	370.41
		0.01	369.94	366.98	366.68	43.08	40.95	38.43	10.28	9.78	9.15
		0.025	362.06	358.71	357.52	23.14	21.76	20.12	7.21	6.81	6.32
		0.05	329.24	325.93	322.91	14.41	13.43	12.26	5.53	5.20	4.80
		0.1	245.92	236.50	224.34	9.02	8.33	7.50	4.27	3.98	3.66
		0.25	74.46	65.67	55.81	5.00	4.54	4.00	3.02	2.85	2.63
		0.5	15.10	12.17	9.00	3.27	2.94	2.55	2.34	2.11	1.98
		1	3.67	2.86	2.05	2.16	1.94	1.69	1.96	1.89	1.69
		2	1.49	1.17	1.01	1.47	1.17	1.01	1.47	1.17	1.01
		4	1.00	1.00	1.00	1.00	1.00	1.00	1.00	1.00	1.00
	Student's t	0	370.31	370.75	370.81	370.66	370.54	370.49	370.24	370.82	370.83
		0.01	364.88	369.49	371.30	34.46	32.36	29.67	8.65	8.15	7.57

Table 2 (continued)

Chart	Distribution	δ	Shift			Linear drift			Quadratic drift		
			$n=5$	$n=7$	$n=10$	$n=5$	$n=7$	$n=10$	$n=5$	$n=7$	$n=10$
		0.025	355.23	355.40	351.03	17.87	16.58	15.06	6.02	5.64	5.19
		0.05	316.32	310.28	296.84	10.91	10.03	9.00	4.62	4.30	3.91
		0.1	215.43	197.69	170.57	6.76	6.14	5.42	3.57	3.27	2.96
		0.25	39.66	31.49	22.45	3.71	3.30	2.85	2.58	2.26	2.02
		0.5	5.71	4.26	2.87	2.42	2.10	1.82	1.98	1.94	1.80
		1	1.79	1.34	1.05	1.68	1.32	1.05	1.68	1.32	1.05
		2	1.00	1.00	1.00	1.00	1.00	1.00	1.00	1.00	1.00
		4	1.00	1.00	1.00	1.00	1.00	1.00	1.00	1.00	1.00
	Gamma	0	370.56	370.70	370.32	370.62	370.21	370.90	370.34	370.95	370.48
		0.01	424.26	431.56	415.87	53.56	51.66	48.20	11.19	10.60	9.87
		0.025	487.66	502.88	478.40	27.58	26.27	24.30	7.82	7.34	6.77
		0.05	524.19	525.53	496.31	16.78	15.77	14.39	6.00	5.60	5.13
		0.1	433.26	413.58	381.00	10.36	9.56	8.57	4.64	4.31	3.86
		0.25	172.05	158.51	131.81	5.67	5.11	4.45	3.28	2.96	2.82
		0.5	30.00	26.03	19.16	3.69	3.28	2.79	2.73	2.30	1.99
		1	4.75	3.60	2.44	2.50	2.07	1.86	1.99	1.97	1.86
		2	1.86	1.41	1.00	1.84	1.41	1.00	1.84	1.41	1.00
		4	1.00	1.00	1.00	1.00	1.00	1.00	1.00	1.00	1.00

lower ARL_1 value indicates sensitivity of the chart, enabling quicker identification of drifts and prompting administrators to intervene and make necessary adjustments, thereby improving the quality of the process. The performance evaluations of CUSUM charts under zero-state monitoring with respect to subgroup sizes $n = 5$, 7, and 10 are shown in Table 2 for normal, student's t, and Gamma distributions. The findings are explained as follows:

- Under normal distribution, the $\overline{X}-$CUSUM chart performance is superior in spotting shifts and drifts. In Table 2, at $n = 5$ and $0.025\sigma_0$ change (shift), the ARL_1 value of the $\overline{X}-$CUSUM chart is decreasing by 12.94 units, while in the $\widetilde{X}-$CUSUM chart, a reduction of 8.66 units in ARL_1 values were observed. At $n = 7$ and $0.25\sigma_0$ change (linear drift), the ARL_1 value of $\overline{X}-$CUSUM chart equals 4.03 while the ARL_1 value of $\widetilde{X}-$CUSUM chart equals 4.54. In the case of quadratic drift at $n = 10$, the $\overline{X}-$CUSUM chart has $ARL_1 = 1.93$ and the $\widetilde{X}-$CUSUM chart has $ARL_1 = 1.98$ for $0.5\sigma_0$ change.
- Under the student's t distribution, the $\widetilde{X}-$CUSUM charts have lower ARL_1 values. It outperforms the $\overline{X}-$CUSUM chart at detecting drifts. In Table 2 at $n = 5$ and $0.025\sigma_0$ change (shift), for example, the ARL_1 value of $\overline{X}-$CUSUM chart is decreasing by 9.91 units, while in the $\widetilde{X}-$CUSUM chart, there was a 15.08 unit decrease in ARL_1 values. The ARL_1 value of the $\overline{X}-$CUSUM chart equals 6.56 for $0.1\sigma_0$ change in the linear drift case with $n = 7$, while the ARL_1 value of the $\widetilde{X}-$CUSUM chart is 6.14. Moreover, in the case of quadratic drift at $n = 10$, the $\overline{X}-$CUSUM chart has $ARL_1 = 1.92$ and the $\widetilde{X}-$CUSUM chart has $ARL_1 = 1.80$ for $0.5\sigma_0$ change.
- Under Gamma distribution, the performance of the $\overline{X}-$CUSUM is more effective in detecting and adapting to drifts in the data. It is able to accurately identify changes in the process, even when there are variations in the average run length ARL due to bias in both charts. The bias appears when $0.01 \leq \delta \leq 0.1$; authors such as Riaz [42] and Lee et al. [43] mentioned related appearances. In Table 2, at $n = 5$ when $\delta = 0.025$ (shift), the ARL_1 values have increased by 70.68 units in the $\overline{X}-$CUSUM chart while the ARL_1 value of the $\widetilde{X}-$CUSUM chart has increased by 117.1 units. At $n = 7$ when $\delta = 0.25$ (linear drift), the $\widetilde{X}-$CUSUM chart has $ARL_1 = 5.11$ but the $\overline{X}-$CUSUM chart has $ARL_1 = 4.75$. At $n = 10$ when $\delta = 0.5$ (quadratic drift), the $\overline{X}-$CUSUM chart has $ARL_1 = 1.98$ and the $\widetilde{X}-$CUSUM chart has $ARL_1 = 1.99$.
- The subgroup size influences the ability of the control chart to identify drifts. An accurate picture of the process is given by the larger subgroup size, which makes it easier to spot minor drifts. Therefore, the size of the subgroup should be decided in light of the unique requirements and characteristics of the process being observed. In the Gamma distribution $\overline{X}-$CUSUM chart, as an example, the ARL_1

Table 3 Steady-state ARL profile of $\overline{X}-$ CUSUM and $\widetilde{X}-$ CUSUM charts when $n = 5,7$, and 10

Chart	Distribution	δ	Shift			Linear drift			Quadratic drift		
			$n=5$	$n=7$	$n=10$	$n=5$	$n=7$	$n=10$	$n=5$	$n=7$	$n=10$
$\overline{X}$	Normal	0	370.03	370.64	370.89	370.77	370.45	370.87	370.61	370.67	370.48
		0.01	366.26	370.35	367.61	82.43	80.59	78.86	55.41	54.83	54.40
		0.025	358.24	360.30	358.27	65.66	64.51	63.55	52.80	52.46	52.16
		0.05	332.12	326.64	323.27	58.51	57.64	56.87	51.43	51.12	50.83
		0.1	249.75	242.34	232.21	54.16	53.53	53.00	50.42	50.09	49.85
		0.25	102.24	95.07	88.74	50.82	50.39	50.02	49.39	49.22	48.99
		0.5	56.88	54.83	53.03	49.40	49.15	48.87	48.77	48.61	48.57
		1	49.28	48.75	48.21	48.67	48.40	48.12	48.64	48.37	48.12
		2	47.93	47.76	47.79	47.92	47.81	47.79	47.91	47.74	47.74
		4	47.80	47.72	47.71	47.82	47.74	47.74	47.83	47.76	47.80
	Student's t	0	370.97	370.91	370.98	370.49	370.11	370.89	370.64	370.78	370.90
		0.01	365.87	371.35	368.27	79.00	77.44	75.62	54.74	54.31	53.82
		0.025	361.76	362.31	361.06	63.50	62.44	61.24	52.27	52.12	51.67
		0.05	341.17	340.34	331.89	56.99	56.24	55.51	51.05	50.77	50.48
		0.1	272.14	262.95	247.40	53.12	52.61	52.11	50.20	49.93	49.65
		0.25	93.57	86.38	78.08	50.29	50.04	49.60	49.21	49.03	48.68
		0.5	52.71	51.29	50.12	49.17	48.88	48.63	48.66	48.62	48.59
		1	48.59	48.21	47.85	48.45	48.20	47.83	48.44	48.25	47.82
		2	47.80	47.82	47.65	47.76	47.75	47.75	47.74	47.75	47.66
		4	47.78	47.72	47.73	47.77	47.78	47.75	47.76	47.73	47.77
	Gamma	0	370.53	370.67	370.72	370.82	370.87	370.10	370.19	370.79	370.15
		0.01	400.00	400.52	394.65	90.51	88.05	85.37	56.34	55.77	55.25
		0.025	431.74	429.85	419.66	69.75	67.97	66.47	53.51	53.07	52.56
		0.05	448.26	445.16	421.28	60.70	59.65	58.56	51.93	51.54	51.21
		0.1	380.85	362.08	335.83	55.47	54.64	53.98	50.81	50.43	50.14
		0.25	165.27	148.61	131.92	51.55	51.02	50.60	49.61	49.36	49.28
		0.5	67.11	62.31	58.34	49.93	49.50	49.17	49.12	48.73	48.52
		1	50.40	49.49	48.78	48.89	48.61	48.43	48.66	48.61	48.45
		2	48.32	47.86	47.72	48.37	47.94	47.75	48.36	47.90	47.72
		4	47.82	47.77	47.73	47.80	47.80	47.74	47.80	47.75	47.75
$\widetilde{X}$	Normal	0	370.70	370.73	370.26	370.73	370.41	370.82	370.23	370.36	370.50
		0.01	369.56	367.24	369.37	84.86	82.84	80.35	55.98	55.42	54.87
		0.025	360.89	359.33	357.83	67.21	66.07	64.45	53.33	52.93	52.38
		0.05	334.25	331.98	327.86	59.62	58.74	57.56	51.83	51.49	51.12
		0.1	261.17	254.54	243.51	54.90	54.22	53.48	50.75	50.41	50.08
		0.25	112.01	104.29	95.46	51.44	51.00	50.43	49.63	49.50	49.11
		0.5	60.04	57.44	54.64	49.82	49.56	49.10	49.13	48.83	48.62
		1	50.16	49.40	48.68	48.90	48.62	48.41	48.78	48.56	48.34
		2	48.29	47.95	47.82	48.28	47.99	47.75	48.28	47.96	47.69
		4	47.91	47.87	47.72	47.88	47.84	47.77	47.93	47.82	47.80
	Student's t	0	370.19	370.20	370.44	370.50	370.85	370.91	370.66	370.52	370.83
		0.01	365.29	364.42	370.11	77.00	75.07	72.84	54.50	53.93	53.49

Table 3 (continued)

Chart	Distribution	δ	Shift			Linear drift			Quadratic drift		
			$n=5$	$n=7$	$n=10$	$n=5$	$n=7$	$n=10$	$n=5$	$n=7$	$n=10$
		0.025	356.69	354.46	352.48	62.55	61.33	60.01	52.18	51.75	51.40
		0.05	325.31	315.34	305.47	56.40	55.60	54.72	50.93	50.63	50.32
		0.1	234.59	219.39	196.89	52.79	52.31	51.63	49.99	49.69	49.42
		0.25	81.20	73.94	66.53	50.11	49.73	49.36	49.16	48.81	48.68
		0.5	51.76	50.50	49.38	49.01	48.64	48.45	48.60	48.59	48.41
		1	48.38	48.05	47.74	48.36	47.98	47.79	48.33	47.92	47.79
		2	47.70	47.76	47.73	47.78	47.76	47.74	47.78	47.74	47.74
		4	47.73	47.71	47.75	47.76	47.76	47.79	47.84	47.73	47.77
	Gamma	0	370.94	370.03	370.70	370.76	370.78	370.17	370.40	370.39	370.53
		0.01	415.03	423.32	412.48	93.72	91.84	88.88	56.79	56.20	55.42
		0.025	473.19	487.11	463.52	71.12	69.81	67.99	53.79	53.27	52.68
		0.05	504.30	503.91	477.12	61.69	60.71	59.50	52.24	51.82	51.29
		0.1	429.19	411.17	379.55	56.00	55.22	54.33	51.04	50.70	50.24
		0.25	197.28	186.06	162.53	52.00	51.34	50.68	49.81	49.46	49.32
		0.5	72.84	69.46	63.61	50.18	49.70	49.30	49.32	48.91	48.57
		1	51.04	49.99	48.94	49.16	48.69	48.45	48.73	48.59	48.44
		2	48.55	48.08	47.66	48.51	48.04	47.67	48.50	48.12	47.67
		4	47.88	47.69	47.71	47.83	47.77	47.72	47.84	47.74	47.67

values at $0.5\sigma_0$ (shift scenario) are 23.36, 17.81, and 13.27 in $n = 5,\ 7,$ and 10, respectively.

5.2 Steady-State Run Length Performance

The discussion in this section will spotlight how CUSUM control charts performed during steady-state monitoring. The ARL_1 values are given so that the performance of the charts can be compared in Table 3. The distributions, including the normal, student's t, and Gamma distributions, were assessed with regard to subgroup sizes $n = 5$, 7, and 10. Thus, the information shown in Table 3 is interpreted as follows:

- Under normal distribution, the $\overline{X}-$CUSUM chart is more efficient in spotting different kinds of shifts and drifts compared to the other chart. In Table 3, at $n = 5$ and $0.025\sigma_0$ change (shift), the ARL_1 value of the $\overline{X}-$CUSUM chart indicated a reduction of 11 units, but the reduction in the $\widetilde{X}-$CUSUM chart was actually 9.47 units. At $n = 7$ and $0.25\sigma_0$ change (linear drift), the ARL_1 value of $\overline{X}-$CUSUM chart has reduced by 320.06 units while ARL_1 value of $\widetilde{X}-$CUSUM chart has reduced by 319.45. At $n = 10$ and $0.5\sigma_0$ change (quadratic drift), the $\overline{X}-$CUSUM chart has $ARL_1 = 48.57$ and the $\widetilde{X}-$CUSUM chart has $ARL_1 = 48.62$
- Under the student's t distribution, the $\widetilde{X}-$CUSUM has a high ability to detect shifts and drifts due to the fact that it displays the lowest value of ARL_1. In Table 3 at $n = 5$ and $0.025\sigma_0$ change (shift), the decrease in units in ARL_1 value of $\overline{X}-$CUSUM chart is 9.21 units; while, the ARL_1 values in the $\widetilde{X}-$CUSUM chart is reduced by 13.5 units. At $n = 7$ and $0.25\sigma_0$ change (linear drift), the ARL_1 value of $\overline{X}-$CUSUM chart has reduced by 320.07 units while ARL_1 value of $\widetilde{X}-$CUSUM chart has reduced by 321.12. At $n = 10$ and $0.5\sigma_0$ change (quadratic drift), the $\overline{X}-$CUSUM chart has $ARL_1 = 48.59$ and $\widetilde{X}-$CUSUM chart has $ARL_1 = 48.41$.
- Under Gamma distribution, at $0.01 \leq \delta \leq 0.1$, both charts show biased behavior under shifting scenarios, but similar biases are not observed for drift scenarios. Despite biases, the $\overline{X}-$CUSUM chart still demonstrates a good performance in detecting shifts and drifts. In Table 3, at $n = 5$ (shift), the $0.1\sigma_0$ change may increase the ARL_1 values of the $\overline{X}-$CUSUM chart by 10.32 units, but in the $\widetilde{X}-$CUSUM chart, the same change may raise the ARL_1 values by 58.25 units. At $n = 7$ and $0.25\sigma_0$ change (linear drift), the $\overline{X}-$CUSUM chart $ARL_1 = 51.02$ but $\widetilde{X}-$CUSUM chart has $ARL_1 = 51.34$. At $n = 10$ and $0.5\sigma_0$ change (quadratic drift), $\overline{X}-$CUSUM chart has $ARL_1 = 48.52$ and $\widetilde{X}-$CUSUM chart has ARL_1 equal to 48.57.

Table 4 Superiority Zones of $\overline{X}-$CUSUM and $\widetilde{X}-$CUSUM Control Charts under different states, distributional environment, sample size, shift and drifts (i.e., Linear and Quadratic drifts)

State	Distribution	n	Shift	Linear drift	Quadratic drift
Zero-state	Normal	5	$\overline{X}-$CUSUM		
		7			
		10			
	Student's t	5	$\widetilde{X}-$CUSUM		
		7			
		10			
	Gamma	5	$\overline{X}-$CUSUM with biased results when $\delta \leq 0.1$		
		7			
		10			
Steady-state	Normal	5	$\overline{X}-$CUSUM		
		7			
		10			
	Student's t	5	$\widetilde{X}-$CUSUM		
		7			
		10			
	Gamma	5	$\overline{X}-$CUSUM with biased results when $\delta \leq 0.1$		
		7			
		10			

- The subgroup size contributes to the drift detection of the control chart. In the normal distribution, the $\widetilde{X}-$CUSUM chart, as an example, the ARL_1 values at $0.1\sigma_0$ change (quadratic drift) are 50.75, 50.41, and 50.08 in $n = 5,7$, and 10, respectively.

Overall, according to the results of zero-state and steady-state monitoring for shifts and drifts, the $\overline{X}-$CUSUM chart and $\widetilde{X}-$CUSUM chart performs better when zero-state monitoring is taken into consideration. When there is quadratic drift in the process, the $\overline{X}-$CUSUM chart and the $\widetilde{X}-$CUSUM chart performs even better. The choice between the two depends on the underlying distribution of process, with the $\overline{X}-$CUSUM chart suitable for normal and Gamma distributions, with a higher ability to detect drifts under biased and unbiased ARLs when it comes to linear drift and quadratic drift (cf. Table 4). Whereas the $\widetilde{X}-$CUSUM chart excels under the student's t distribution (cf. Table 4). However, both charts are faster at spotting quadratic drifts than linear ones. Additionally, for both charts, the value of ARL_1 drops as n rises. In other words, the $\overline{X}-$CUSUM and $\widetilde{X}-$CUSUM charts become more sensitive to detecting drifts as the sample size increases.

6 Comparative Analysis Under Drifts

In this section, we demonstrate how the CUSUM charts, EWMA charts, and Shewhart charts performed in zero- and steady-state monitoring. Table 5 and Figs. 1 and 2 provide the results of the CUSUM charts (i.e., $\overline{X}-$CUSUM and $\widetilde{X}-$CUSUM), the EWMA control charts (i.e., the $\overline{X}-$EWMA and $\widetilde{X}-$EWMA charts), and Shewhart control charts (i.e., the $\overline{X}$ and $\widetilde{X}$ charts). The ARL_1 values are compared to the δ values, which are predefined thresholds such as 0.01, 0.025, 0.05, 0.1, 0.25, 0.5, 1, 2, and 4. The results are taken at $n = 10$ since increasing the subgroup size significantly affects the ability to detect abnormalities. Ultimately, the chart with the lowest ARL_1 value is considered the best in terms of performance evaluation. Figures 1 and 2 characterize the ARL curves of the control charts based on the sample mean and sample median. In Fig. 1, plots A, B, and C represent normal, student's t, and Gamma distributions, respectively, under zero-state monitoring; while, plots D, E, and F represent the same distributions but under steady-state monitoring in the presence of linear and quadratic drifts monitoring. On the other hand, the ARL Curves of the control charts, based on the sample median in Fig. 2 represented by plots A, B, and C, represent normal, student's t, and Gamma distributions, respectively, under zero-state monitoring. In contrast, plots D, E, and F represent the same distributions

Table 5 ARL profile of CUSUM charts with EWMA charts and Shewhart charts when $n = 10$

State	Distribution	δ	Linear drift						Quadratic drift					
			$\overline{X}-$ CUSUM	EWMA$_{\overline{X}}$	$\overline{X}$	$\widetilde{X}-$ CUSUM	EWMA$_{\widetilde{X}}$	$\widetilde{X}$	$\overline{X}-$ CUSUM	EWMA$_{\overline{X}}$	$\overline{X}$	$\widetilde{X}-$ CUSUM	EWMA$_{\widetilde{X}}$	$\widetilde{X}$
Zero-state monitoring	Normal	0	370.97	370.03	370.80	370.77	370.86	370.88	370.43	370.71	370.54	370.41	370.37	370.50
		0.01	36.51	26.47	42.05	38.43	29.39	47.52	8.71	8.36	9.22	9.15	8.88	9.89
		0.025	18.96	14.75	21.91	20.12	16.36	24.88	5.98	5.99	6.25	6.32	6.36	6.70
		0.05	11.47	9.63	13.12	12.26	10.63	14.95	4.52	4.68	4.65	4.80	4.96	4.99
		0.1	6.94	6.36	7.79	7.50	7.00	8.89	3.44	3.69	3.50	3.66	3.89	3.73
		0.25	3.64	3.77	3.90	4.00	4.13	4.44	2.42	2.78	2.42	2.63	2.89	2.61
		0.5	2.28	2.61	2.34	2.55	2.84	2.64	1.93	2.01	1.92	1.98	2.09	1.96
		1	1.47	1.95	1.44	1.69	2.00	1.64	1.47	1.95	1.43	1.69	1.98	1.62
		2	1.00	1.06	1.00	1.01	1.27	1.01	1.00	1.06	1.00	1.01	1.27	1.01
		4	1.00	1.00	1.00	1.00	1.00	1.00	1.00	1.00	1.00	1.00	1.00	1.00
	Student's t	0	370.82	370.03	370.36	370.49	370.59	370.60	370.42	370.66	370.15	370.83	370.17	370.12
		0.01	32.88	22.06	42.67	29.67	20.34	34.14	8.01	7.47	8.72	7.57	7.17	7.97
		0.025	16.56	12.27	21.34	15.06	11.40	17.40	5.52	5.37	5.85	5.19	5.16	5.38
		0.05	9.88	8.02	12.42	9.00	7.49	10.23	4.18	4.19	4.35	3.91	4.03	4.01
		0.1	5.97	5.32	7.17	5.42	5.00	6.01	3.15	3.27	3.22	2.96	3.13	2.99
		0.25	3.16	3.18	3.48	2.85	3.01	2.98	2.14	2.37	2.14	2.02	2.21	2.02
		0.5	2.00	2.14	2.05	1.82	2.05	1.81	1.92	1.99	1.90	1.80	1.99	1.78
		1	1.18	1.69	1.16	1.05	1.48	1.05	1.18	1.70	1.15	1.05	1.48	1.05
		2	1.00	1.00	1.00	1.00	1.00	1.00	1.00	1.00	1.00	1.00	1.00	1.00
		4	1.00	1.00	1.00	1.00	1.00	1.00	1.00	1.00	1.00	1.00	1.00	1.00
	Gamma	0	370.58	370.78	370.18	370.90	370.86	370.31	370.51	370.70	370.20	370.48	370.34	370.95
		0.01	44.14	29.57	57.23	48.20	30.34	61.65	9.55	8.76	10.66	9.87	8.81	11.09
		0.025	22.47	16.30	29.59	24.30	16.53	31.85	6.56	6.26	7.14	6.77	6.30	7.40
		0.05	13.41	10.50	17.53	14.39	10.56	18.85	4.98	4.87	5.29	5.13	4.84	5.46
		0.1	8.06	6.86	10.24	8.57	6.83	10.96	3.79	3.83	3.90	3.86	3.78	4.01
		0.25	4.24	4.03	4.96	4.45	3.96	5.27	2.76	2.88	2.76	2.82	2.85	2.83
		0.5	2.69	2.78	2.87	2.71	2.72	3.03	1.98	2.02	1.98	1.99	2.00	1.98
		1	1.81	1.97	1.77	1.86	1.95	1.84	1.81	1.97	1.77	1.86	1.95	1.84

Table 5 (continued)

State	Distribution	δ	Linear drift						Quadratic drift					
			$\overline{X}$ – CUSUM	EWMA$_{\overline{X}}$	$\overline{X}$	$\widetilde{X}$ – CUSUM	EWMA$_{\widetilde{X}}$	$\widetilde{X}$	$\overline{X}$ – CUSUM	EWMA$_{\overline{X}}$	$\overline{X}$	$\widetilde{X}$ – CUSUM	EWMA$_{\widetilde{X}}$	$\widetilde{X}$
		2	1.00	1.16	1.00	1.00	1.05	1.00	1.00	1.16	1.00	1.00	1.06	1.00
		4	1.00	1.00	1.00	1.00	1.00	1.00	1.00	1.00	1.00	1.00	1.00	1.00
Steady-state monitoring	Normal	0	370.87	370.57	370.75	370.82	370.16	370.81	370.48	370.82	370.70	370.50	370.65	370.91
		0.01	78.86	70.35	83.62	80.35	72.99	87.97	54.40	54.57	54.81	54.87	55.05	55.59
		0.025	63.55	60.08	66.01	64.45	61.49	68.30	52.16	52.47	52.27	52.38	52.86	52.66
		0.05	56.87	55.61	58.31	57.56	56.51	59.59	50.83	51.36	50.88	51.12	51.68	51.26
		0.1	53.00	52.85	53.60	53.48	53.41	54.44	49.85	50.47	49.96	50.08	50.64	50.16
		0.25	50.02	50.56	50.25	50.43	50.85	50.64	48.99	49.67	48.96	49.11	49.83	49.14
		0.5	48.87	49.55	48.88	49.10	49.77	49.01	48.57	48.99	48.49	48.62	49.22	48.61
		1	48.12	48.88	48.10	48.41	48.94	48.10	48.12	48.84	48.10	48.34	48.93	48.26
		2	47.79	48.31	47.72	47.75	48.48	47.60	47.74	48.30	47.67	47.69	48.44	47.72
		4	47.74	48.13	47.70	47.77	48.12	47.64	47.80	48.16	47.70	47.80	48.18	47.66
	Student's t	0	370.89	371.99	370.87	370.91	370.70	370.17	371.90	370.83	370.27	370.83	370.96	370.94
		0.01	75.62	66.40	83.25	72.84	65.06	76.47	53.82	53.72	83.23	53.49	53.54	53.92
		0.025	61.24	57.87	65.11	60.01	57.09	61.84	51.67	51.89	64.99	51.40	51.77	51.62
		0.05	55.51	54.18	57.47	54.72	53.73	55.69	50.48	50.83	57.49	50.32	50.74	50.39
		0.1	52.11	51.79	52.94	51.63	51.57	51.98	49.65	50.01	52.92	49.42	49.99	49.52
		0.25	49.60	49.97	49.74	49.36	49.78	49.29	48.68	49.28	49.82	48.68	49.19	48.60
		0.5	48.63	49.03	48.57	48.45	49.02	48.34	48.59	48.87	48.51	48.41	48.88	48.42
		1	47.83	48.57	47.78	47.79	48.52	47.64	47.82	48.54	47.80	47.79	48.56	47.82
		2	47.75	48.03	47.71	47.74	48.15	47.59	47.66	48.04	47.63	47.74	48.07	47.81
		4	47.75	48.00	47.66	47.79	48.14	47.62	47.77	48.07	47.66	47.77	48.15	47.74
	Gamma	0	371.10	370.59	370.92	370.17	370.58	370.28	370.15	370.00	371.83	370.53	370.50	370.93
		0.01	85.37	73.09	96.31	88.88	73.75	100.86	55.25	54.92	56.18	55.42	54.97	56.50
		0.025	66.47	61.55	72.49	67.99	61.84	74.81	52.56	52.79	53.10	52.68	52.77	53.34
		0.05	58.56	56.43	62.11	59.50	56.62	63.45	51.21	51.47	51.45	51.29	51.55	51.63
		0.1	53.98	53.25	55.76	54.33	53.36	56.43	50.14	50.58	50.33	50.24	50.59	50.40

Table 5 (continued)

State	Distribution	δ	Linear drift						Quadratic drift					
			$\overline{X}-$ CUSUM	EWMA$_{\overline{X}}$	$\overline{X}$	$\widetilde{X}-$ CUSUM	EWMA$_{\widetilde{X}}$	$\widetilde{X}$	$\overline{X}-$ CUSUM	EWMA$_{\overline{X}}$	$\overline{X}$	$\widetilde{X}-$ CUSUM	EWMA$_{\widetilde{X}}$	$\widetilde{X}$
		0.25	50.60	50.72	51.20	50.68	50.78	51.38	49.28	49.77	49.26	49.32	49.72	49.33
		0.5	49.17	49.66	49.36	49.30	49.71	49.48	48.52	49.08	48.53	48.57	49.07	48.60
		1	48.43	48.93	48.39	48.45	48.92	48.49	48.45	48.94	48.34	48.44	48.85	48.51
		2	47.75	48.36	47.73	47.67	48.41	47.74	47.72	48.33	47.74	47.67	48.40	47.70
		4	47.74	48.10	47.70	47.72	48.13	47.69	47.75	48.14	47.72	47.67	48.15	47.81

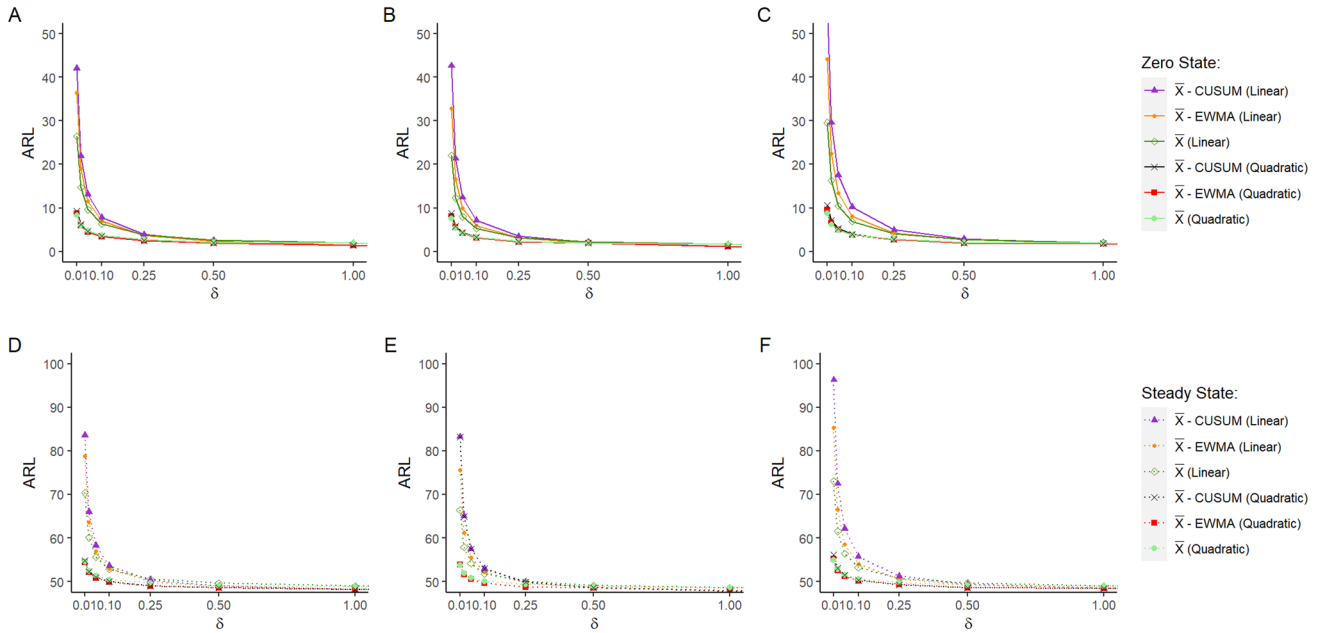

Fig. 1 ARL Curves of the control charts based on sample mean in presence of linear and quadratic drifts. The first plots representing zero-state: **a** Normal distribution, **b** Student t distribution, and **c** gamma distribution. The last plots representing steady-state: **d** Normal distribution, **e** Student t distribution, and **f** gamma distribution

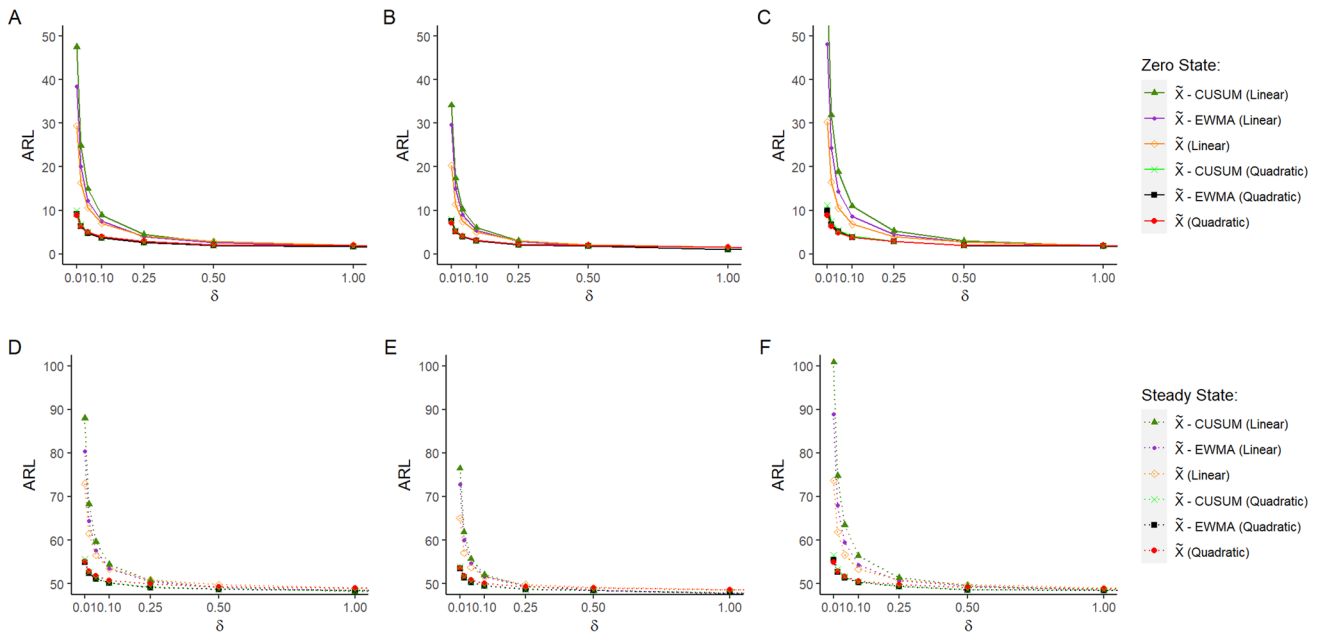

Fig. 2 ARL Curves of the control charts based on sample median in presence of linear and quadratic drifts. The first plots representing zero-state: **a** Normal distribution, **b** Student t distribution, and **c** gamma distribution. The last plots representing steady-state: **d** Normal distribution, **e** Student t distribution, and **f** gamma distribution

under steady-state monitoring in the presence of linear and quadratic drifts.

The results are explained as follows, starting with the zero-state monitoring:

- Under normal distribution (cf. Figures 1a and 2a), in terms of detecting the linear drift, the $\overline{X}$ − CUSUM and $\widetilde{X}$ − CUSUM charts provide lower ARL_1 values when $\delta \geq 0.25$ compared to the $\overline{X}$ − EWMA and $\widetilde{X}$ − EWMA charts that provide lower ARL_1 values when δ is between 0.01 and 0.1. But the superiority goes to the Shewhart $\overline{X}$ and $\widetilde{X}$ charts when $\delta \geq 1$, since Shewhart charts are constructed to detect a high number of shifts and drifts. For instance, at δ =0.25, the ARL_1 values for the $\overline{X}$ − CUSUM and $\widetilde{X}$ − CUSUM charts are reported as 3.64 and 4, respectively, while the ARL_1 values for the $\overline{X}$−EWMA and $\widetilde{X}$−EWMA charts are 3.77 and 4.13, respectively. The ARL_1 values for the $\overline{X}$ and $\widetilde{X}$ charts equal 3.90 and 4.44, respectively.
- In terms of identifying the quadratic drift, $\overline{X}$−CUSUM and $\widetilde{X}$−CUSUM chart has a better performance when $0.025 \leq \delta < 0.5$ compared to $\overline{X}$ − EWMA and $\widetilde{X}$ − EWMA charts that provide lower ARL_1 values only when $\delta = 0.01$. However, when $\delta \geq 0.5$, Shewhart charts perform better at spotting quadratic drifts. For example, at δ =0.25, the ARL_1 values for the $\overline{X}$−CUSUM and $\widetilde{X}$−CUSUM charts are reported as 2.42 and 2.63, respectively, while the ARL_1 values for the $\overline{X}$−EWMA and $\widetilde{X}$−EWMA charts are 2.78 and 2.89, respectively. The ARL_1 values for the $\overline{X}$ and $\widetilde{X}$ charts equal 3.90 and 2.61, respectively.
- Under the student's t distribution (cf. Figures 1b and 2b, in terms of detecting linear drift, the $\overline{X}$ − CUSUM and $\widetilde{X}$ − CUSUM charts provide lower ARL_1 values when $0.25 \leq \delta < 1$ compared to the $\overline{X}$ − EWMA and $\widetilde{X}$ − EWMA charts that provide lower ARL_1 values when δ is between 0.01 and 0.1. Generally, the superiority goes to Shewhart $\overline{X}$ chart when $\delta \geq 1$, and for the $\widetilde{X}$ chart only when $\delta = 0.5$. For example, at$\delta = 0.25$, the ARL_1 values for the $\overline{X}$−CUSUM and $\widetilde{X}$−CUSUM charts equal 3.16 and 2.85, respectively, but for the $\overline{X}$ − EWMA and $\widetilde{X}$ − EWMA charts are reported as 3.18 and 3.01, respectively. The ARL_1 values for the $\overline{X}$ and $\widetilde{X}$ charts equal 3.48 and 2.98, respectively. In terms of identifying the quadratic drift, $\overline{X}$ − CUSUM and $\widetilde{X}$ − CUSUM charts perform better when $0.05 \leq \delta < 1$ compared to $\overline{X}$ − EWMA and $\widetilde{X}$ − EWMA charts that provide lower ARL_1 values only when$\delta = 0.01 and 0.025$. However, when$\delta \geq 1$, Shewhart charts perform better at spotting quadratic drifts. For example, at$\delta = 0.1$, the ARL_1 values for the $\overline{X}$ − CUSUM and $\widetilde{X}$ − CUSUM charts are reported as 3.15 and 2.96, respectively, while the ARL_1 values for $\overline{X}$ − EWMA and $\widetilde{X}$ − EWMA charts are 3.27 and 3.13, respectively. The ARL_1 values for the $\overline{X}$ and $\widetilde{X}$ charts equal 3.22 and 2.99, respectively. It is worth noting that all of the statistics that are based on the sample median outperform the ones that are based on the sample mean.
- Under Gamma distribution (cf. Figures 1c and 2c), in terms of detecting linear drift, the $\overline{X}$−CUSUM and $\widetilde{X}$−CUSUM charts exhibit an improvement in drift detection when $0.5 \leq \delta < 2$ compared to the $\overline{X}$−EWMA and $\widetilde{X}$−EWMA charts that performs better when δ is $0.01 \leq \delta \leq 0.25$ and chart when δ is between 0.01 and 0.5 and for Shewhart $\overline{X}$ and $\widetilde{X}$ charts when $\delta \geq 2$. For instance, at δ =0.25, the ARL_1 values for the $\overline{X}$−CUSUM and $\widetilde{X}$−CUSUM charts are reported as 3.64 and 4, respectively, while the ARL_1 values for the $\overline{X}$−EWMA and $\widetilde{X}$−EWMA charts are 3.77 and 4.13, respectively. The ARL_1 values for the $\overline{X}$ and $\widetilde{X}$ charts equal 3.90 and 4.44, respectively. In terms of identifying the quadratic drift, $\overline{X}$−CUSUM and $\widetilde{X}$−CUSUM chart has a better performance when $0.1 \leq \delta < 1$ compared to $\overline{X}$ − EWMA and $\widetilde{X}$ − EWMA charts that provide lower ARL_1 values only when $\delta = 0.01$, 0.025 and 0.05. However, when $\delta \geq 1$, Shewhart charts perform better at spotting quadratic drifts. For example, at δ =0.25, the ARL_1 values for the $\overline{X}$−CUSUM and $\widetilde{X}$−CUSUM charts are reported as 2.76 and 2.82, respectively, while the ARL_1 values for $\overline{X}$ − EWMA and $\widetilde{X}$ − EWMA charts are 2.88 and 2.85, respectively. The ARL_1 values for the $\overline{X}$ and $\widetilde{X}$ charts equal 2.76 and 2.83, respectively. However, at $\delta = 0.25 and 0.5$, the ARL_1 values for the $\overline{X}$ − CUSUM is reporting similar behavior to Shewhart control charts under specific drift values.

Now that steady-state monitoring is taken into account, the following conclusions are explained:

- Under normal distribution (cf. Figures 1d and 2d), $\overline{X}$ − CUSUM chart and $\widetilde{X}$ − CUSUM provides lower ARL_1 values compared to Shewhart $\overline{X}$ and $\widetilde{X}$ charts with the same drift range (i.e., $0.01 \leq \delta \leq 0.5$). Therefore, the superiority goes to the $\overline{X}$−CUSUM and $\widetilde{X}$−CUSUM chart in detecting the drifts. Meanwhile, $\overline{X}$−CUSUM chart and $\widetilde{X}$ − CUSUM provides lower ARL_1 values compared to $\overline{X}$ − EWMA and $\widetilde{X}$ − EWMA charts when $0.25 \leq \delta \leq 0.5$. In order to detect the quadratic drift, $\overline{X}$ − CUSUM and $\widetilde{X}$ − CUSUM chart better than to $\overline{X}$ − EWMA and $\widetilde{X}$ − EWMA charts the $\overline{X}$ and $\widetilde{X}$ charts. For example, at 0.1σ, the ARL_1 value of the $\overline{X}$−CUSUM chart and for $\overline{X}$ chart are reported as 49.85 and 49.96. On the other hand, the ARL_1 value of the $\widetilde{X}$ − CUSUM chart is reported as 50.08; whereas, the $\widetilde{X}$ chart is 50.16 at $\delta = 0.01$. For example, at 0.05 σ, the values of the $\overline{X}$ − CUSUM chart and $\widetilde{X}$ − CUSUM charts are 50.83 and 51.12, respectively, while the ARL_1 values of the $\overline{X}$ − EWMA and $\widetilde{X}$ − EWMA charts equal 51.36 and 51.68, respectively. However, Shewhart charts, which are constructed to detect

Table 6 Superiority Zones of CUSUM, EWMA, and Shewhart Control Charts under Linear and Quadratic Drifts

State	Distribution	Charts	Linear drift	Quadratic drift
Zero-state	Normal	EWMA	$0.01 \leq \delta \leq 0.1$	$\delta = 0.01$
		CUSUM	$0.25 \leq \delta < 1$	$0.025 \leq \delta < 0.5$
		Shewhart	$\delta \geq 1$	$\delta \geq 0.5$
	Student's t	EWMA	$0.01 \leq \delta \leq 0.1$	$0.01 \leq \delta \leq 0.025$
		CUSUM	$0.25 \leq \delta < 1$	$0.05 \leq \delta < 1$
		Shewhart	$\delta \geq 1$	$\delta \geq 1$
	Gamma	EWMA	$0.01 \leq \delta \leq 0.25$	$0.01 \leq \delta \leq 0.05$
		CUSUM	$0.5 \leq \delta < 2$	$0.1 \leq \delta < 1$
		Shewhart	$\delta \geq 2$	$\delta \geq 1$
Steady-state	Normal	EWMA	$0.01 \leq \delta \leq 0.1$	–
		CUSUM	$0.25 \leq \delta < 1$	$0.01 \leq \delta < 0.5$
		Shewhart	$\delta \geq 1$	$\delta \geq 0.5$
	Student's t	EWMA	$0.01 \leq \delta \leq 0.1$	–
		CUSUM	$0.25 \leq \delta < 1$	$0.01 \leq \delta < 0.5$
		Shewhart	$\delta \geq 1$	$\delta \geq 0.5$
	Gamma	EWMA	$0.01 \leq \delta \leq 0.1$	$\delta = 0.01$
		CUSUM	$0.25 \leq \delta < 1$	$0.025 \leq \delta < 0.5$
		Shewhart	$\delta \geq 1$	$\delta \geq 0.5$

a high-magnitude drift, perform better in spotting the drifts when δ becomes higher than $0.5\sigma_0$ both drift types.

- Under the student's t distribution (cf. Figures 1e and 2e), in terms of detecting linear drift, the $\overline{X}$ − CUSUM and $\widetilde{X}-$CUSUM charts provide lower ARL_1 values when $\delta = 0.25$ compared to the $\overline{X}-$EWMA and $\widetilde{X}-$EWMA charts that provide lower ARL_1 values when δ is between 0.01 and 0.1. Generally, the superiority goes to the Shewhart $\overline{X}$ chart when $\delta \geq 1$, and for the $\widetilde{X}$ chart only when $\delta \geq 0.5$. In terms of identifying the quadratic drift, $\overline{X}-$CUSUM and $\widetilde{X}-$CUSUM charts perform better when $\delta \geq 0.025$ compared $\overline{X}-$EWMA and $\widetilde{X}-$EWMA charts that provide lower ARL_1 values only when $\delta = 0.01$. However, when $\delta \geq 0.5$, Shewhart charts perform better at spotting quadratic drifts. For example, at $\delta = 0.1$, the ARL_1 values for the $\overline{X}-$CUSUM and $\widetilde{X}-$CUSUM charts are reported as 49.65 and 49.42, respectively, while the ARL_1 values for $\overline{X}-$EWMA and $\widetilde{X}-$EWMA charts are 50.01 and 49.99, respectively. The ARL_1 values for the $\overline{X}$ and $\widetilde{X}$ charts equal 52.92 and 49.52, respectively. Under the steady-state monitoring scenario, the superiority goes to the $\widetilde{X}-$CUSUM chart since it provides lower ARL_1 values.
- Under Gamma distribution (cf. Figures 1f and 2f), in terms of detecting linear drift, the CUSUM charts show improved drift detection when $\delta \geq 0.25$ compared to the EWMA charts, which perform better when $\delta \leq 0.1$, and the Shewhart charts. The CUSUM charts outperform the other charts when quadratic drifts are present at $\delta > 0.01$. However, superiority goes to the $\overline{X}-$CUSUM chart in detecting the drifts. For example, the $\overline{X}-$CUSUM and $\widetilde{X}-$CUSUM charts have ARL_1 values equal to 49.28 and 49.32, respectively, when $\delta = 0.25$. While the ARL_1 values for the $\overline{X}-$EWMA and $\widetilde{X}-$EWMA charts are 49.77 and 49.72, respectively, and for the $\overline{X}$ and $\widetilde{X}$ chart the ARL_1 values equal 49.26 and 49.33, respectively.

The figures clearly indicate that the performance of charts improved in terms of identifying the quadratic drift. Some charts differ in their ability to locate drifts in different ranges of δ, so the choice of which chart to use depends on factors such as the desired detection speed and the type of drift being monitored. Additionally, it is important to consider the distributional settings and whether a zero-state scenario is applicable.

Based on the results from zero- and steady-state presented in Table 6, it can be concluded that $\overline{X}-$CUSUM and $\widetilde{X}-$CUSUM charts outperform Shewhart charts when δ is between 0.01 and 0.5 and exceed EWMA charts when $\delta \geq 0.25$. The $\overline{X}-$CUSUM is also better suited to identifying drifts in normal and Gamma distributions. While the $\widetilde{X}-$CUSUM chart is effective at locating drifts within the student's environment. The slight linear drifts (i.e., $0.01 \leq \delta \leq 0.1$) are detected by EWMA charts before the quadratic one under all distributional settings. The charts using the sample median are faster at detecting quadratic drifts compared to the ones using the sample mean under the student's t distribution. The drifts will be identified quickly under the

Table 7 List of acronyms

ARL	Average Run Length	UCL	Upper Control Limit
ARL_0	In-control Average Run Length	μ	Mean
ARL_1	Out-of-Control Average Run Length	μ_0	In-control Mean
CL	Central Limit	μ_1	Out-of-Control Mean
CUSUM	Cumulative Sum	N	Normal Distribution
EWMA	Exponentially Weighted Moving Average	n	Sample Size
$\overline{X}-$ CUSUM	Cumulative Sum of Mean	τ	Change Point
$\widetilde{X}-$ CUSUM	Cumulative Sum of Median	k	Reference Value
FAR	False Alarm Rate	h_1	Charting constant for Lower Control Limit
IC	In-control	h_2	Charting constant for Upper Control Limit
LCL	Lower Control Limit	t	Time Point
$MDRL$	Median of Run Length	δ	Amount of Shift
OOC	Out-of-Control	σ	Standard Deviation
RL	Run Length	σ_0	In-control Standard Deviation
$SDRL$	Standard Deviation of Run Length	σ_1	Out-of-Control Standard Deviation
SPC	Statistical Process Control	X	Random Variable

zero-state scenario (Fig. 1). The charts detect quadratic drift faster than the linear ones (Fig. 2). The choice of which chart to use depends on the specific characteristics of the drift being monitored. Table 5 provides a concise summary of the optimal parameters for each control chart method under various drift conditions, facilitating users in selecting the most effective control chart for their specific monitoring requirements (Table 7).

7 Real-life Illustrations

In this section, two real-life examples are used to show the implementation of the proposed charts.

8 A Nitrogen Oxides Concentration Level Illustration

A dataset of air quality in an Italian town was taken from the UCI Machine Learning Repository [44]. This data was collected from five metal oxide chemistry sensors, including CO concentration, non-Metonic hydrocarbons, benzene, total nitrogen oxides (NOx), and nitrogen dioxide. The dataset was recorded for a year from March 2004 to April 2005. NOx is the variable of interest for monitoring because it is the most dangerous factor for human and environmental health, which causes respiratory tract damage, increased infection susceptibility, asthma, chronic lung illness, irritation, and lung tissue destruction. In the preliminary computation stage, missing values of NOx levels have been eliminated. The total number of observations was 7718; however, we eliminated the last three to consider only 7715. Based on this, we grouped them into groups of five subsamples, yielding a total of 1543 groupings. Using the break-point procedure provided by the "segmented" R package, there were 607 observations under control; while, the rest were not in Fig. 3a, b. Then, for each subgroup of 5, the $\overline{X}-$CUSUM and $\widetilde{X}-$CUSUM were determined. From the regression analysis, the fitted model of the NOx is defined as $NOx = -2618 + 6.377\text{t} - 0.003351\text{t}^2$, which indicated that the OOC data drifted quadratically in Fig. 3c, d. Furthermore, The Shapiro–Wilk test with the PP-plots implies that the variables might not have a normal distribution but instead adhere to a gamma distribution Fig. 3e, f.

The baseline performance of the process was determined by analyzing the data. This required computing the mean and standard deviation of data points in order to set control limits. For the $\overline{X}-$CUSUM chart, the IC mean and the standard deviation are determined to be 128.76 and 63.50, respectively. Moreover, the control limits LCL and UCL of the chart are set to 0 and 1.371, respectively, and the reference value equals $k = 0.5$. In terms of being able to detect quadratic drift, $\tau = 222$, the $\overline{X}-$CUSUM chart Fig. 4a was able to detect the drift at sample number 223. Likewise, the IC mean and standard deviation of the $\widetilde{X}-$CUSUM are set to be 126.54 and 71.92, respectively. Also, the LCL and UCL of the chart are set to 0 and 1.997, respectively. In terms of the ability to identify quadratic drift, $\tau = 354$, the $\widetilde{X}-$CUSUM chart Fig. 4c was able to detect the drift at sample number 362. As a result, the $\overline{X}-$CUSUM detects quadratic drift more effectively compared to $\widetilde{X}-$CUSUM, which matches the findings of our study.

8.1 A Case Study on Maintenance Data

Another example of the suggested charts is shown using actual predictive maintenance data. [45]. The dataset was collected in 2020, has a total of 10,000 samples, and shows a

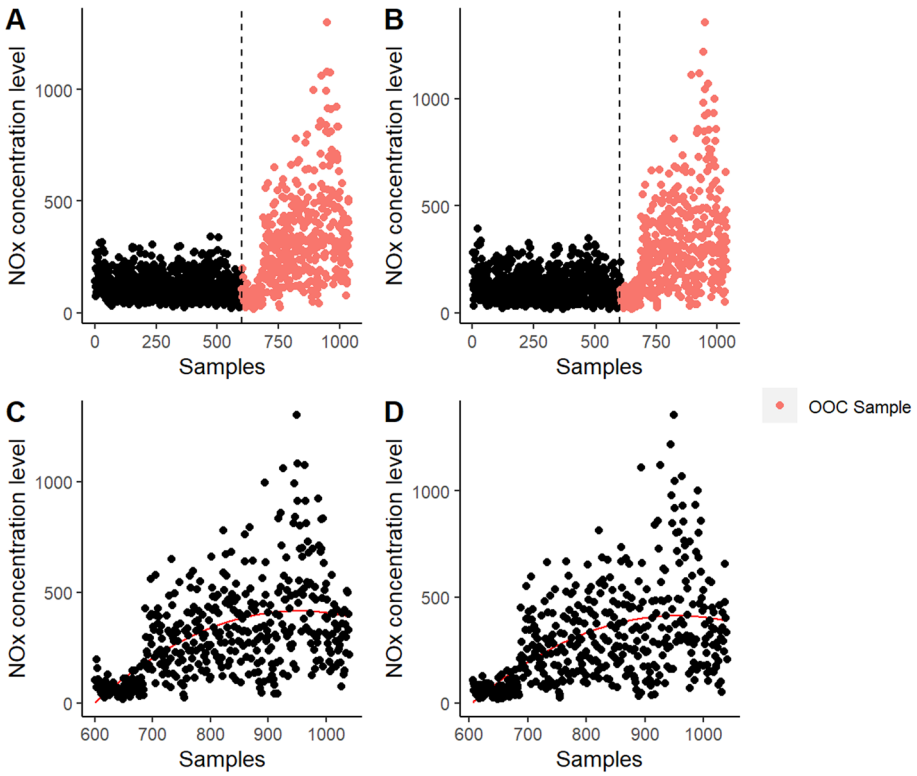

Fig. 3 Scatter plot for the IC and OOC data of the NOx concentration level; **a** $\overline{X}$ values, **b** $\widetilde{X}$ values, **c**for OOC $\overline{X}$ with the quadratic trend, and **d** for OOC $\widetilde{X}$ with the quadratic trend, **e** PP-plot for the IC NOx concentration level $\overline{X}$ values, and **f** PP-plot for the IC NOx concentration level $\widetilde{X}$ values

variety of factors that might influence the operation, including air temperature, rotating speed, and equipment failure. Predictive maintenance keeps an eye on the performance of equipment during ordinary operations and searches for any anomalies that could indicate a probable breakdown. One of the most important elements impacting preventative maintenance is the process temperature. In actuality, it is routinely employed as a crucial indicator of machinery health. Because of this, the variable of importance in this example is process temperature. For the illustration, we have only taken into account the 5200 observations. Data are separated into subgroups of size 5 for the preprocessing stage. Using the break-point procedure provided by the "segmented" R package, we have further divided the data into "in-control" IC data, which consists of the first 375 samples, and "out-of-control" OOC data, which includes the remaining observations Fig. 5a, b. The mean and median are determined for each subgroup. We used regression to determine if the OOC data drifted quadratically or linearly, and the results showed that the data drifted quadratically in Fig. 5c, d.

Furthermore, The Shapiro–Wilk test with the pp-plots implies that the variables have a normal distribution in Fig. 5e, f. The fitted regression model was Temperature $= 350.70 + 0.006457t + 0.00000177t^2$. By examining the data, the baseline performance of the process was established. Setting control limits required calculating the mean and standard deviation of the data points. The IC mean and the standard deviation for $\overline{X}-$CUSUM chart is found to be $\overline{X} = 297.67$ and $\sigma_{\overline{X}} = 0.879$. Aside from that, the control limits LCL and UCL of chart are set at 0 and 1.001, respectively, and the reference value is set at $k = 0.5$. Regarding the ability to identify the drift, $\tau = 56$, the $\overline{X}-$CUSUM chart Fig. 6a was able to detect the drift at sample number 83. Similarly, the $\widetilde{X}-$CUSUM IC mean, and standard deviation are set to 297.67 and 0.878, respectively. The LCL and UCL of chart are further set to 0 and 1.0017, respectively. Since $\tau = 70$, the $\widetilde{X}-$CUSUM chart Fig. 6c was able to detect the drift at sample number 98. Consequently, the $\overline{X}-$CUSUM chart identifies quadratic drift faster than $\widetilde{X}-$CUSUM, which is consistent with the results of our investigation.

9 Conclusions and Future Recommendations

This study aimed to investigate the detection behavior of CUSUM charts in the presence of linear and quadratic drifts. We assessed the performance of CUSUM charts based on sample mean and median across various distributions and subgroup sizes under zero and steady-state monitoring conditions. Our findings underscore the significant influence of subgroup size on chart performance, emphasizing the need to balance accuracy and sensitivity in selecting appropriate subgroup sizes for process monitoring. Notably, our

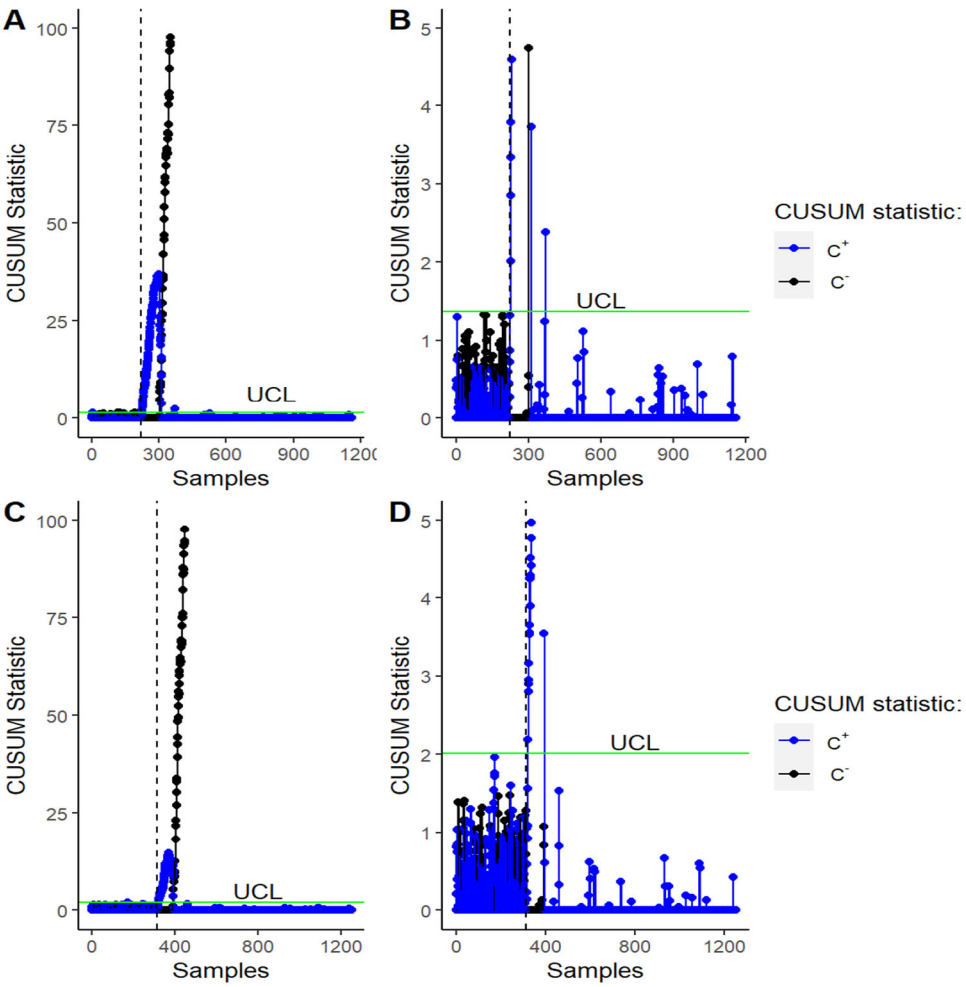

Fig. 4 **a** the $\overline{X}$ − CUSUM chart, **b** the zoomed $\overline{X}$ − CUSUM chart, **c** the $\widetilde{X}$ − CUSUM chart and **d** the zoomed $\widetilde{X}$ − CUSUM charts for NOx level

study revealed the superiority of CUSUM charts in zero-state monitoring and their effectiveness in detecting quadratic drifts. Depending on the underlying distribution, the Mean-CUSUM chart excels in normal and Gamma distributions, while the Median-CUSUM chart outperforms in the student's t distribution.

Comparative analysis with EWMA and Shewhart charts highlighted the effectiveness of CUSUM charts for detecting drifts within specific drift sizes. Focusing on linear and quadratic drifts, our study provides valuable insights into process monitoring methods, with practical applications demonstrated in air quality and maintenance data scenarios. We acknowledge that our study has limitations, including the scope restricted to linear and quadratic drifts and the need for further exploration of other drift types. Also, the whole study was designed under the restriction to univariate setups. Future research should explore multivariate setups to enhance the applicability of CUSUM charts in complex manufacturing environments. Additionally, while our study assumed a known population model, future investigations should consider distribution-free setups to accommodate nonparametric environments.

In this paper, we aim to study the detection behavior of CUSUM chart in the presence of linear drift and quadratic drift. The performance of the $\overline{X}$ − CUSUM chart and $\widetilde{X}$ − CUSUM chart as location charts is being assessed, taking into consideration that $\overline{X}$ and $\widetilde{X}$ are the plotting statistics. The performance of charts is evaluated into various distributions and subgrouping sizes under two monitoring states (i.e., zero and steady-states). The study reveals that the size of the subgroup can significantly influence the performance of control chart. For instance, a smaller subgroup size (i.e., $n = 5$) may make the control chart less sensitive to small process drifts, suggesting the need to balance accuracy and sensitivity when selecting the appropriate subgroup size for monitoring a process. The CUSUM charts perform better when zero-state monitoring is considered. They are more effective when quadratic drift is present. Depending on the underlying distribution, the $\overline{X}$ − CUSUM chart is appropriate for normal and Gamma distributions. It has a high ability to detect linear and quadratic drift under biased and unbiased ARLs. Meanwhile,

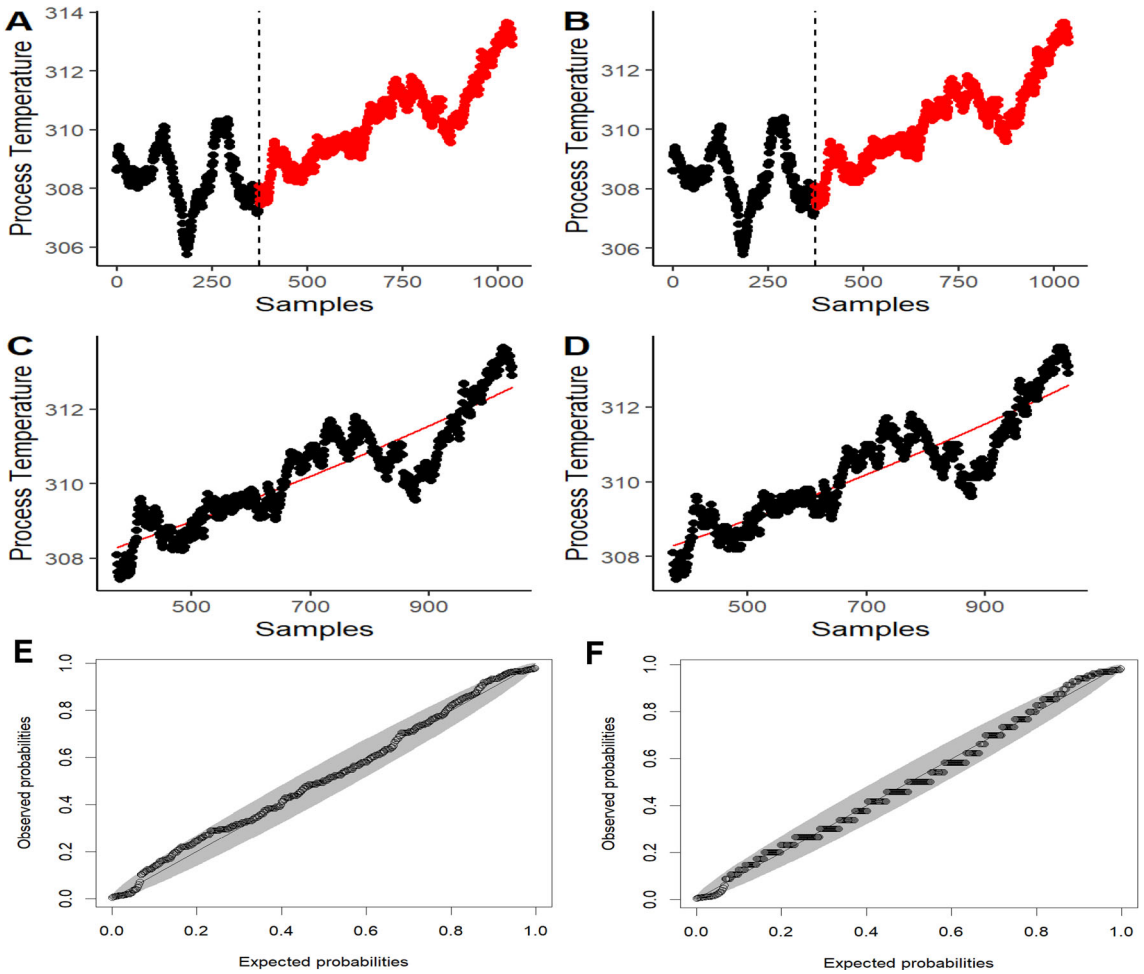

Fig. 5 Scatter plot for the IC and OOC data for the temperature of maintenance dataset; **a** $\overline{X}$ values, **b** $\widetilde{X}$ values, **c** for OOC $\overline{X}$ with the quadratic trend, and **d** for OOC $\widetilde{X}$ with the quadratic trend, (E) PP-plot for the IC process temperature $\overline{X}$ values, and (F) PP-plot for the IC process temperature $\widetilde{X}$ values

$\widetilde{X}-$ CUSUM excels under the student's t distribution and is faster at spotting quadratic drifts. A comparable analysis of detection performance was conducted using the CUSUM charts, EWMA charts, and Shewhart charts. The comparative analysis (Sect. 5.1) revealed that the Shewhart charts are more effective in detecting larger drifts in the process as they are designed for. However, based on the findings from zero- and steady-state, it can be concluded that the $\overline{X}-$ CUSUM and $\widetilde{X}-$ CUSUM charts are superior to the Shewhart charts for δ between 0.01 and 0.5 and the EWMA charts for $\delta \geq 0.25$. The $\overline{X}-$CUSUM is better suited for identifying drifts in normal and Gamma distributions, while the $\widetilde{X}-$ CUSUM chart is superior in the student's t distribution. The sample median charts are faster at detecting quadratic drifts than the sample mean under the student's t distribution. Moreover, EWMA charts have a higher sensitivity to detecting quite minor (i.e., between 0.01 and 0.1) in the process mean, making them more effective for early detection. EWMA charts detect slight linear drifts before the quadratic one under all distributional settings. Therefore, depending on the desired level of sensitivity and the magnitude of potential drifts, either chart can be chosen for monitoring process drifts effectively. The proposed charts are deployed in real-life scenarios related to air quality and maintenance data. Additionally, the CUSUM performance is comparable to the EWMA and Shewhart control charts in terms of the number of signals produced. This study assessed effects of drifts on the CUSUM chart with respect to location parameters but could extend to other memory-type dispersion charts. The discussion in this paper only covers linear and quadratic drift, but it could be expanded to cover other types of drift.

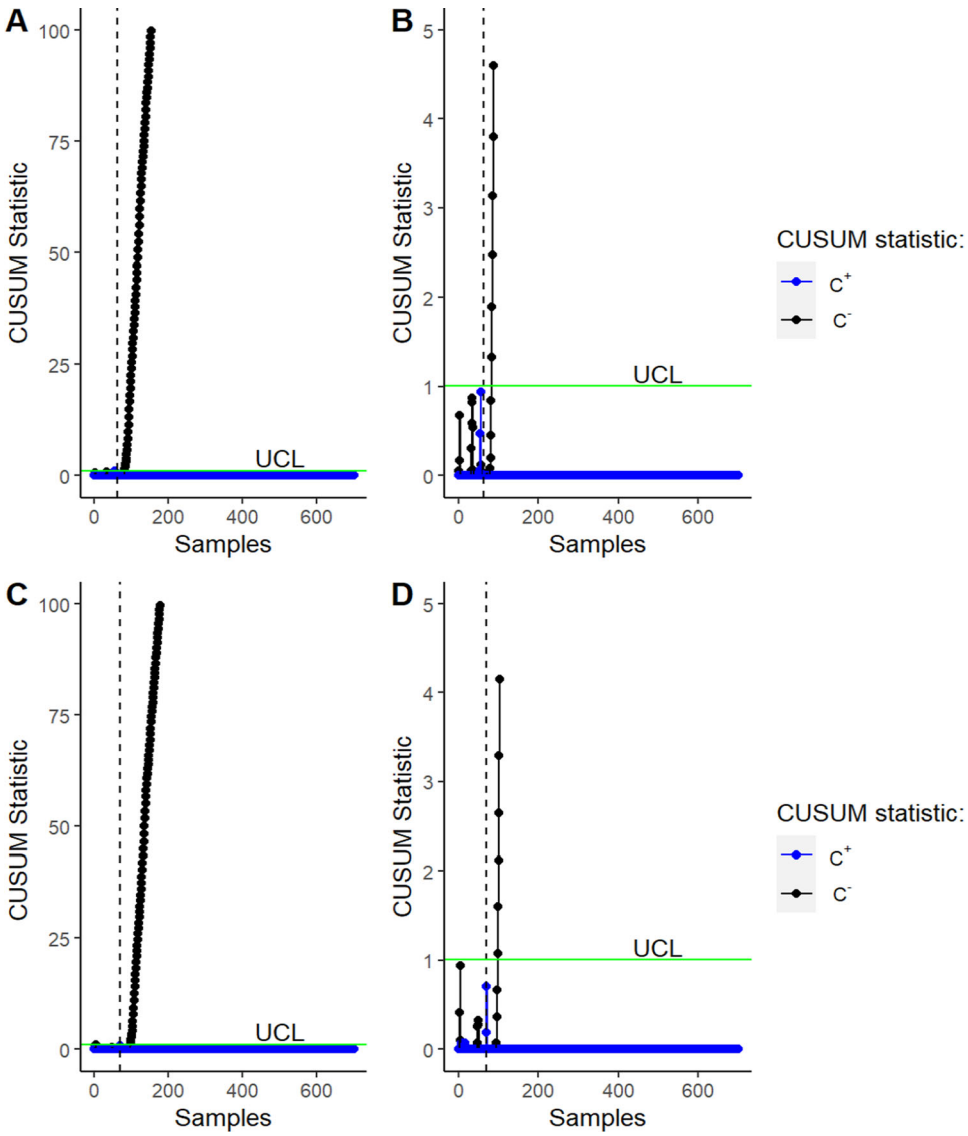

Fig. 6 **a** the $\overline{X}$ − CUSUM chart, **b** Zoomed the $\overline{X}$ − CUSUM chart, **c** the $\widetilde{X}$ − CUSUM charts and **d** Zoomed the $\widetilde{X}$ − CUSUM charts of the temperature

References

1. Mahmood, T.: Generalized linear modelling based monitoring methods for air quality surveillance. J. King Saud Univ. Sci. **36**(4), 103145 (2024)
2. Montgomery DC. Introduction to statistical quality control. John Wiley & Sons; 2020.
3. Page, E.S.: Continuous Inspection Schemes. Biometrika **41**(1/2), 100–115 (1954). https://doi.org/10.2307/2333009
4. Tran, P.H., Nguyen, H.D., Heuchenne, C., Tran, K.P.: Monitoring Coefficient of Variation Using CUSUM Control Charts. Springer handbook of engineering statistics. Springer; 2023. pp. 333–360.
5. Erem, A., Mahmood, T.: A bivariate CUSUM control chart based on exceedance statistics. Qual. Reliab. Eng. Int. **39**(4), 1172–91 (2023). https://doi.org/10.1002/qre.3285
6. Abbas, N.: On efficient change point detection using a step cumulative sum control chart. Qual. Eng. **35**(4), 712–728 (2023)
7. Chakraborti, S.; Graham, M.A.: Nonparametric (distribution-free) control charts: an updated overview and some results. Qual. Eng. **31**(4), 523–544 (2019)
8. Madrid-Alvarez, H.M.; García-Díaz, J.C.; Tercero-Gómez, V.G.: A CUSUM control chart for gamma distribution with guaranteed performance. Qual. Reliab. Eng. Int. **40**(3), 1279–1301 (2024)
9. Özdemir, A.; Uçurum, M.; Serencam, H.: A novel fuzzy cumulative sum control chart with an α-level cut based on trapezoidal

fuzzy numbers for a real case application. Arab. J. Sci. Eng. **49**, 7507–7525 (2024)
10. Reynolds, M.R.; Stoumbos, Z.G.: Individuals control schemes for monitoring the mean and variance of processes subject to drifts. SAA. **19**(5), 863–892 (2001). https://doi.org/10.1081/SAP-120000226
11. Bissell, A.F.: Estimation of linear trend from a cusum chart or tabulation. R. Stat. Soc. Ser. C (Appl. Stat) **33**(2), 152–157 (1984). https://doi.org/10.2307/2347440
12. Bissell, A.F.: The Performance of control charts and cusums under linear trend. R. Stat. Soc. Ser. C (Appl. Stat.) **33**(2), 145–151 (1984). https://doi.org/10.2307/2347439
13. Aerne, L.A.; Champ, C.W.; Rigdon, S.E.: Evaluation of control charts under linear trend. Commun. Stat. Theory Methods **20**(10), 3341–3349 (1991). https://doi.org/10.1080/03610929108830706
14. Gan, F.F.: Ewma control chart under linear drift. JSCS. **38**(1–4), 181–200 (1991). https://doi.org/10.1080/00949659108811328
15. Davis, R.B.; Krehbiel, T.C.: Shewhart and zone control chart performance under linear trend. Commun. Stat. Simul. Comput. **31**(1), 91–96 (2002)
16. Bücher, A.; Fermanian, J.D.; Kojadinovic, I.: Combining cumulative sum change-point detection tests for assessing the stationarity of univariate time series. J. Time Ser. Anal. **40**(1), 124–150 (2019)
17. Hou, S.; Yu, K.: A non-parametric CUSUM control chart for process distribution change detection and change type diagnosis. Int. J. Prod. Res. **59**(4), 1166–1186 (2021)
18. Diko, M.D.; Chakraborti, S.; Does, R.J.: An alternative design of the two-sided CUSUM chart for monitoring the mean when parameters are estimated. Comput. Ind. Eng. **137**, 106042 (2019)
19. Haq, A.; Ali, Q.: A maximum dual CUSUM chart for joint monitoring of process mean and variance. Qual. Technol. Quant. Manage. **21**(3), 287–308 (2024)
20. Gültekin, M.; English, J.R.; Elsayed, E.A.: Cross-correlation and X-bar -trend control charts for processes with linear shift. IJPR. **40**(5), 1051–1064 (2002). https://doi.org/10.1080/00207540110102133
21. Fahmy, H.M.; Elsayed, E.A.: Drift time detection and adjustment procedures for processes subject to linear trend. IJPR. **44**(16), 3257–3278 (2006). https://doi.org/10.1080/00207540500410242
22. Shu, L.; Jiang, W.; Tsui, K.-L.: A Weighted CUSUM chart for detecting patterned mean shifts. JQT. **40**(2), 194–213 (2008). https://doi.org/10.1080/00224065.2008.11917725
23. Zou, C.; Liu, Y.; Wang, Z.: Comparisons of control schemes for monitoring the means of processes subject to drifts. Metrika **70**(2), 141–163 (2009). https://doi.org/10.1007/s00184-008-0183-6
24. Yi, F.; Qiu, P.: An adaptive CUSUM chart for drift detection. Qual. Reliab. Eng. Int. **38**(2), 887–894 (2022)
25. Mejri, D.; Limam, M.; Weihs, C.: A new time adjusting control limits chart for concept drift detection. IFAC J. Syst. Control. **17**, 100170 (2021)
26. Mou, Z.; Chiang, J.-Y.; Chen, S.; Liu, G.: A likelihood-based adaptive CUSUM for monitoring linear drift of Poisson rate with time-varying sample sizes. J. Stat. Comput. Simul. (2024). https://doi.org/10.1080/00949655.2024.2327376
27. Capizzi, G.; Masarotto, G.: Guaranteed in-control control chart performance with cautious parameter learning. J. Qual. Technol. **52**(4), 385–403 (2020)
28. Assareh, H.; Smith, I.; Mengersen, K.: Bayesian estimation of the time of a linear trend in risk-adjusted control charts. Int. J. Adv. Manuf. Technol. **38**(4), 409–417 (2011)
29. Atashgar, K.; Noorossana, R.: An integrating approach to root cause analysis of a bivariate mean vector with a linear trend disturbance. Int. J. Adv. Manuf. Technol. **52**(1), 407–420 (2011). https://doi.org/10.1007/s00170-010-2728-x
30. Xu, L.; Wang, S.; Reynolds, M.R., Jr.: A generalized likelihood ratio control chart for monitoring the process mean subject to linear drifts. Int. J. Adv. Manuf. Technol. **29**(4), 545–553 (2013). https://doi.org/10.1002/qre.1404
31. Yi, F.; Qiu, P.: An adaptive CUSUM chart for drift detection. Qual. Reliabil. Eng. Int. **38**(2), 887–894 (2022). https://doi.org/10.1002/qre.3020
32. Centofanti, F.; Lepore, A.; Menafoglio, A.; Palumbo, B.; Vantini, S.: Functional regression control chart. Technometrics **63**(3), 281–294 (2021). https://doi.org/10.1080/00401706.2020.1753581
33. Lefebvre, W.; Miller, E.: Linear-quadratic stochastic delayed control and deep learning resolution. J. Opt. Theory Appl. **191**(1), 134–168 (2021). https://doi.org/10.1007/s10957-021-01923-x
34. Han, B.; Pun, C.S.; Wong, H.Y.: Robust time-inconsistent stochastic linear-quadratic control with drift disturbance. Appl. Math. Optim. **86**(1), 4 (2022)
35. Li, N.; Li, X.; Peng, J.; Xu, Z.Q.: Stochastic linear quadratic optimal control problem: a reinforcement learning method. ITAC. **67**(9), 5009–5016 (2022). https://doi.org/10.1109/TAC.2022.3181248
36. Marais, H.L.; Zaccaria, V.; Odlare, M.: Comparing statistical process control charts for fault detection in wastewater treatment. Water Sci. Technol. **85**(4), 1250–1262 (2022). https://doi.org/10.2166/wst.2022.037
37. De Oliveira, B.N.; Valk, M.; Marcondes, F.D.: Fault detection and diagnosis of batch process dynamics using ARMA-based control charts. J. Process. Control. **111**, 46–58 (2022). https://doi.org/10.1016/j.jprocont.2022.01.005
38. Sepp, A.; Rakhmonov, P.: Log-normal stochastic volatility model with quadratic drift. Int J Theoretical Appl Finance. **26**(08), 2450003 (2023). https://doi.org/10.1142/S0219024924500031
39. Maritz, J.S.; Jarrett, R.G.: A note on estimating the variance of the sample median. J Amer Statistical Assoc. **73**(361), 194–196 (1978). https://doi.org/10.1080/01621459.1978.10480027
40. Aslam, M.Z.; Amin, M.; Mahmood, T.; Nauman, A.M.: Shewhart ridge profiling for the Gamma response model. J. Stat. Comput. Simul. (2023). https://doi.org/10.1080/00949655.2023.2299354
41. Amin, M.; Noor, A.; Mahmood, T.: Beta regression residuals-based control charts with different link functions: an application to the thermal power plants data. Int. J. Data Sci. Anal. (2024). https://doi.org/10.1007/s41060-023-00501-w
42. Riaz, M.: Improved and robust monitoring in statistical process control. Universiteit van Amsterdam [Host]; (2008)
43. Lee, P.-H.; Torng, C.-C.; Lin, C.-H.; Chou, C.-Y.: Control chart pattern recognition using spectral clustering technique and support vector machine under gamma distribution. Comput. Ind. Eng. **171**, 108437 (2022)
44. UCI Machine Learning Repository (2016). https://doi.org/10.24432/C59K5F
45. UCI Machine Learning Repository (2020). https://doi.org/10.24432/C5HS5C